

CONTRIBUTION FROM THE DEPARTMENT OF CHEMISTRY,  
MASSACHUSETTS INSTITUTE OF TECHNOLOGY, CAMBRIDGE, MASSACHUSETTS 02139

# Intramolecular Rearrangement Reactions of Tris-Chelate Complexes.

## II.<sup>1</sup> Kinetics and Probable Mechanism of the Isomerization and Racemization of the "Fast" Complexes

### Tris(1-phenyl-5-methylhexane-2,4-dionato)aluminum(III) and -gallium(III)

By J. R. HUTCHISON,<sup>2</sup> J. G. GORDON, II,<sup>3</sup> AND R. H. HOLM\*

Received July 15, 1970

Rearrangement reactions of the title complexes,  $M(\text{pmhd})_3$  (2), have been investigated by proton resonance in chlorobenzene solution. These reactions were found to be intramolecular and to involve geometrical isomerization and inversion of the molecular configuration. The two processes occur simultaneously and were examined by means of the temperature dependencies of isopropyl methyl signals. Experimental spectra in the intermediate-exchange regions of both complexes were compared with those computed for various rearrangement mechanisms of the twist and bond rupture type. Microscopic rate constants for the mechanisms are presented. On the basis of full line shape analysis, a number of mechanisms have been excluded. Those regarded as most probable for  $\text{Al}(\text{pmhd})_3$  and  $\text{Ga}(\text{pmhd})_3$  are certain twist processes and bond rupture to form square-pyramidal-axial transition states. Activation parameters for these mechanisms are given. Tris( $\beta$ -acetyl-pentane-2,4-dionato) complexes of aluminum and gallium were prepared and found not to undergo linkage isomerization at 180° in chlorobenzene. Arguments based on estimated lower limits of the rates of this process compared to the rates of rearrangement of pmhd complexes suggest that  $\text{Ga}(\text{pmhd})_3$  may rearrange by a twist mechanism. Rearrangement rates were found to increase with increasing ionic radius of the metal ion, *viz.*,  $\text{Al} < \text{Ga} \ll \text{Sc}$ .

### Introduction

Determination of the kinetics and pathways of intramolecular rearrangement reactions of metal complexes continues to be one of the most fundamental problems in mechanistic inorganic chemistry. One of the largest and most significant groups of complexes which undergo such reactions is composed of tris chelates.<sup>4</sup> Of this group complexes with the  $M\text{-O}_6$  core, comprised mainly of the tris( $\beta$ -diketonates), constitute a major part. If such complexes contain three unsymmetrical ligands, they can exist in enantiomeric ( $\Delta$ ,  $\Lambda$ ) cis (C) and trans (T) forms as illustrated in Figure 1, and the rearrangement reactions possible are geometrical isomerization and racemization. These reactions can proceed by two types of reaction pathways which are distinguished by the effective coordination number of the transition state. If no metal-ligand bonds are broken, the transition state is an idealized trigonal prism which may be achieved by means of various twist motions of the chelate rings with respect to real or artificial threefold symmetry axes of the cis and trans isomers.<sup>1,5-11</sup> Rupture of one bond leads to a five-coordinate transition state<sup>1,5,7,10</sup> with an idealized trigonal-bipyramidal (TBP) or square-pyramidal (SP) geometry and dangling axial or equatorial (basal) ligands. In the first part<sup>1</sup> of this series a complete analysis of the various bond rupture and twist mechanisms is given, including specification of all transition-state structures or their enantiomers and topological correlation diagrams sum-

marizing the possible interconversions among the four species,  $C\Delta$ ,  $CA$ ,  $T\Delta$ , and  $TA$ , for each mechanism.

It has been demonstrated that accurate determination of the isomerization and racemization rates of the cis and trans isomers can in principle lead to a determination of the mechanism of these reactions provided they both proceed through the same transition state(s).<sup>1</sup> In applying this procedure it is necessary to recognize two limiting types of tris chelates. One type is designated as "slow," indicating that under ordinary conditions geometrical isomers can be completely separated and partially resolved, thereby permitting measurement of isomerization and racemization rates by nmr and polarimetry, respectively. Slow tris( $\beta$ -diketonates) are those formed by the conventionally nonlabile metal ions such as  $\text{Cr(III)}$ ,<sup>12,13</sup>  $\text{Co(III)}$ ,<sup>1,7,12-17</sup>  $\text{Rh(III)}$ ,<sup>7,12,13</sup> and  $\text{Ru(II,III)}$ .<sup>18</sup> The second type is described as "fast," meaning that intramolecular rearrangements are sufficiently rapid to prevent isomer separation or resolution and measurement of rate of approach to equilibrium by these techniques but not necessarily too rapid to disallow isomer detection and measurement of rearrangement kinetics by nmr. Fast tris( $\beta$ -diketonates) are those of the normally labile metal ions, including  $\text{V(III)}$ ,<sup>18,19</sup> high-spin  $\text{Mn(III)}$  and  $\text{Fe(III)}$ ,<sup>12,18,13</sup>  $\text{Al(III)}$ ,<sup>7,9,12-14,20,21</sup>  $\text{Ga(III)}$ ,<sup>7,13,22,23</sup>

(12) R. C. Fay and T. S. Piper, *J. Amer. Chem. Soc.*, **84**, 2303 (1962).(13) R. C. Fay and T. S. Piper, *ibid.*, **85**, 500 (1963).(14) R. A. Palmer, R. C. Fay, and T. S. Piper, *Inorg. Chem.*, **3**, 875 (1964).(15) R. J. York, W. D. Bonds, Jr., B. P. Cotsoradis, and R. D. Archer, *ibid.*, **8**, 789 (1969).(16) J. P. Collman, R. P. Blair, R. L. Marshall, and L. Slade, *ibid.*, **2**, 576 (1963); J. P. Collman and J.-Y. Sun, *ibid.*, **4**, 1273 (1965).

(17) U. Klabunde and R. C. Fay, Abstracts, 156th National Meeting of the American Chemical Society, Sept 1968, No. INOR-37.

(18) J. G. Gordon, II, M. J. O'Connor, and R. H. Holm, *Inorg. Chim. Acta*, in press.(19) F. Röhrscheid, R. E. Ernst, and R. H. Holm, *Inorg. Chem.*, **6**, 1315 (1967).(20) J. A. S. Smith and E. J. Wilkins, *J. Chem. Soc. A*, 1749 (1966).(21) R. G. Linck and R. E. Sievers, *Inorg. Chem.*, **5**, 806 (1966).(22) T. J. Pinnavaia and S. O. Nweke, *ibid.*, **8**, 639 (1969).(23) T. J. Pinnavaia, J. M. Sebeson, II, and D. A. Case, *ibid.*, **8**, 644 (1969).(1) Part I: J. G. Gordon, II, and R. H. Holm, *J. Amer. Chem. Soc.*, **92**, 5319 (1970).

(2) On leave from the Department of Chemistry, Swarthmore College, Swarthmore, Pa., 1969-1970.

(3) National Science Foundation Predoctoral Fellow, 1967-1970.

(4) F. Basolo and R. G. Pearson, "Mechanisms of Inorganic Reactions," 2nd ed, Wiley, New York, N. Y., 1967, pp 300-334.

(5) P. Rây and N. K. Dutt, *J. Indian Chem. Soc.*, **20**, 81 (1943).(6) J. C. Bailar, Jr., *J. Inorg. Nucl. Chem.*, **8**, 165 (1958).(7) R. C. Fay and T. S. Piper, *Inorg. Chem.*, **3**, 348 (1964).(8) C. S. Springer, Jr., and R. E. Sievers, *ibid.*, **6**, 852 (1967).(9) J. J. Fortman and R. E. Sievers, *ibid.*, **6**, 2022 (1967).(10) E. L. Muetterties, *J. Amer. Chem. Soc.*, **90**, 5097 (1968).(11) J. E. Brady, *Inorg. Chem.*, **8**, 1208 (1969).

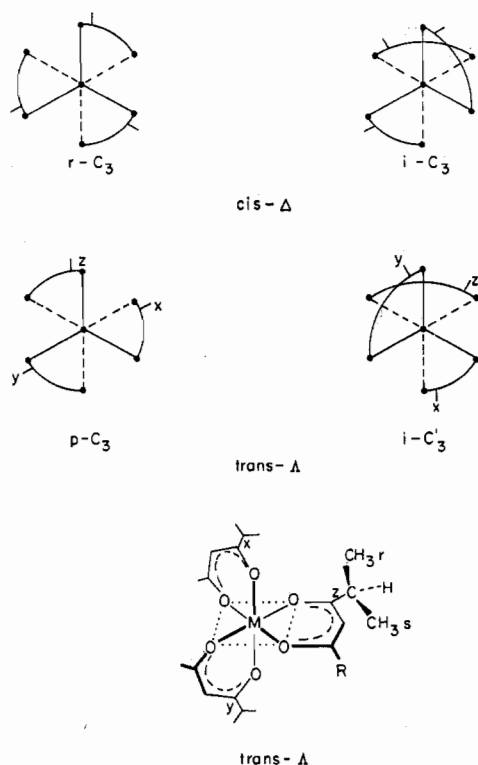


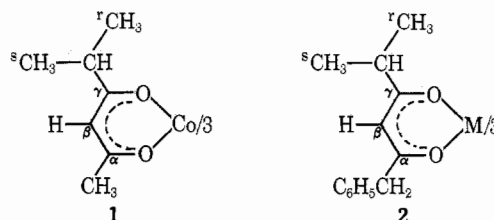
Figure 1.—Top: illustration of cis and trans isomers and  $\Delta, \Lambda$  absolute configurations as viewed down the real (r) and one of the three equivalent imaginary (i) threefold axes of the cis isomers and the pseudo (p) and one of the three inequivalent imaginary (i) threefold axes of the trans isomers. Bottom: illustration of the diastereotopic nature of the  $\gamma$ -*i*-C<sub>3</sub>H<sub>7</sub> methyl groups (r,s) in the trans- $\Delta$  isomer. An absolute stereochemical definition of r and s is not intended.

and In(III).<sup>7,13</sup> The only slow tris( $\beta$ -diketonates) containing central ions without partially filled d shells are those of Si(IV); Si(acac)<sub>3</sub><sup>+</sup> can be resolved<sup>24</sup> and the pmr spectrum of Si(bzac)<sub>3</sub><sup>+</sup><sup>20</sup> is consistent with the presence of geometrical isomers.<sup>25</sup> A similar classification applies to a second group of M-O<sub>6</sub> complexes, formed by tropolone and its derivatives. Al( $\alpha$ -*i*-C<sub>3</sub>H<sub>7</sub>T)<sub>3</sub> and Ga( $\alpha$ -*i*-C<sub>3</sub>H<sub>7</sub>T)<sub>3</sub> are fast<sup>26</sup> whereas SiT<sub>3</sub><sup>+</sup><sup>27</sup> and Si( $\alpha$ -*i*-C<sub>3</sub>H<sub>7</sub>T)<sub>3</sub><sup>+</sup><sup>26</sup> are slow.

Analysis of the experimental isomerization and racemization rates of the slow complex Co(mhd)<sub>3</sub> (1) in chlorobenzene has led to the establishment of a bond rupture mechanism involving a high percentage of TBP-axial transition states.<sup>1</sup> Any detailed study of the rearrangements of fast complexes also necessitates detection of the consequences of racemization and isomerization. This can be accomplished by nmr investigations of such complexes which have the following two properties: (i) suitable substituent groups whose chemical shifts allow detection of geometrical isomers and the chiral nature of each in the slow-exchange

limit and (ii) rates of intramolecular rearrangement such that both the slow- and fast-exchange limits can be attained within the normally accessible temperature range of ca. -70 to +170°.

The complexes of interest in this study are the tris chelates M(pmhd)<sub>3</sub> (2) derived from 1-phenyl-5-methyl-



hexane-2,4-dione, including the slow complex with M = Co(III) and the fast complexes with M = Al(III), Ga(III), and Sc(III). Signals of the  $\beta$  and  $\gamma$  substituents serve to detect the cis and trans forms at slow exchange, under which condition the  $\gamma$ -*i*-C<sub>3</sub>H<sub>7</sub> group senses the chirality of each form. The methyl groups of this substituent are diastereotopic and their consequent magnetic inequivalence, denoted by r and s, is illustrated for trans- $\Delta$  in Figure 1. This paper reports an analysis of the temperature dependence of the pmr spectra of Al(pmhd)<sub>3</sub> and Ga(pmhd)<sub>3</sub>, principally in the isopropyl methyl region, by means of a line shape procedure. Using a kinetic treatment of rearrangements based on that previously derived,<sup>1</sup> line shapes in the intermediate-exchange regions have been computed for the various mechanisms and compared to experimental spectra in an attempt to establish probable reaction mechanisms. Details of the kinetic analysis are presented together with spectral observations of other complexes of type 2. Use of diastereotopic groups to investigate structures and intramolecular processes in organic molecules<sup>28</sup> is now fairly common. Resolution of the magnetic inequivalence of such groups in metal complexes has been infrequently reported, particularly for diamagnetic species, and use of the effect to probe racemization reactions of chelates has been made in only three other cases.<sup>26,29</sup> Of these, Al( $\alpha$ -*i*-C<sub>3</sub>H<sub>7</sub>T)<sub>3</sub> is subject to the same rearrangement reactions as the M-(pmhd)<sub>3</sub> complexes. Analysis of its spectrum<sup>26</sup> has not as yet permitted refinement of mechanistic possibilities.

## Experimental Section

**Preparation of Compounds. 1-Phenyl-5-methylhexane-2,4-dione, H(pmhd).**—This compound was prepared from methylphenylacetate, 3-methyl-2-butanone, and sodium amide in a 2:1:2 molar ratio in ether solution following the procedure of Hauser, *et al.*,<sup>30</sup> for other  $\beta$ -diketonates. Purification was achieved by recrystallization of the copper chelate from ethanol, followed by its decomposition with sulfuric acid and distillation of the resulting liquid. The pure compound was obtained as the fraction boiling at 131–133° (4 mm). *Anal.* Calcd for C<sub>12</sub>H<sub>16</sub>O<sub>2</sub>: C, 76.44; H, 7.89. Found: C, 76.02; H, 7.52.

**Tris(1-phenyl-5-methylhexane-2,4-dionato)aluminum(III), Al(pmhd)<sub>3</sub>.**—The complex was obtained from the reaction of aluminum isopropoxide and H(pmhd) using the procedure for the preparation of Al(bzac)<sub>3</sub>.<sup>12</sup> The crude complex was vacuum

(28) M. van Gorkom and G. E. Hall, *Quart. Rev., Chem. Soc.*, **22**, 14 (1968); K. Mislow and M. Raban, "Topics in Stereochemistry," Vol. 1, N. L. Allinger and E. L. Eliel, Ed., Wiley, New York, N. Y., 1967, Chapter 1.

(29) L. H. Pignolet and R. H. Holm, *J. Amer. Chem. Soc.*, **92**, 1791 (1970); L. H. Pignolet, R. A. Lewis, and R. H. Holm, *ibid.*, **93**, 360 (1971); B. Jurado and C. S. Springer, Jr., *Chem. Commun.*, 85 (1971).

(30) C. R. Hauser, F. W. Swamer, and J. T. Adams, *Org. React.*, **8**, 59 (1954).

(24) S. K. Dhar, V. Doron, and S. Kirschner, *J. Amer. Chem. Soc.*, **81**, 6372 (1959); E. Larsen, S. F. Mason, and G. H. Searle, *Acta Chem. Scand.*, **20**, 191 (1966).

(25) The following abbreviations of  $\beta$ -diketonate anions are employed throughout: acac, acetylacetonate; bzac, benzoylacetonate; dbm, dibenzylmethanide; hfac, hexafluoroacetylacetonate; mhd, 5-methylhexane-2,4-dionate; pmhd, 1-phenyl-5-methylhexane-2,4-dionate; tfac, trifluoroacetylacetonate; triac, triacetylmethanide; also, T, tropolonate.

(26) E. L. Muettterties and C. W. Alegranti, *J. Amer. Chem. Soc.*, **91**, 4420 (1969).

(27) T. Ito, N. Tanaka, I. Hanazaki, and S. Nagakura, *Inorg. Nucl. Chem. Lett.*, **5**, 781 (1969).

distilled (Kugelrohr) from an air bath (255–265°) at 0.15 mm and the product was obtained as a light yellow viscous oil. *Anal.* Calcd for  $C_{39}H_{45}O_6Al$ : C, 73.56; H, 7.12. Found: C, 73.65; H, 7.12.

**Tris(1-phenyl-5-methylhexane-2,4-dionato)gallium(III), Ga(pmhd)<sub>3</sub>.**—A preparation analogous to that for Al(pmhd)<sub>3</sub> was used. Gallium isopropoxide was synthesized according to a published procedure.<sup>31</sup> After vacuum distillation (Kugelrohr) of the crude product at 240–250° (0.15 mm) the compound was obtained as a light yellow viscous oil. *Anal.* Calcd for  $C_{39}H_{45}O_6Ga$ : C, 68.93; H, 6.68. Found: C, 69.10; H, 6.71.

**Tris(1-phenyl-5-methylhexane-2,4-dionato)cobalt(III), Co(pmhd)<sub>3</sub>.**—The complex was prepared from sodium tris(carbonato)cobaltate(III) trihydrate and H(pmhd) and purified following the procedure for Co(mhd)<sub>3</sub>.<sup>1</sup> The mixture of isomers was obtained in the pure state as a green oil. *Anal.* Calcd for  $C_{39}H_{45}O_6Co$ : C, 70.05; H, 6.78. Found: C, 69.73; H, 6.73.

Separation of the complex into its cis and trans isomers was accomplished by chromatography on alumina;<sup>1</sup> the pure cis isomer crystallized on standing.

**Tris(1-phenyl-5-methylhexane-2,4-dionato)scandium(III), Sc(pmhd)<sub>3</sub>.**—A modification of the method of Berg and Acosta<sup>32</sup> for the preparation of other  $\beta$ -diketonate complexes was employed. Solvents were saturated with nitrogen and operations were carried out under nitrogen. A solution of 1.6 g (7.9 mmol) of H(pmhd) in ethanol was neutralized with 0.55 g (8.0 mmol) of sodium ethoxide, and 0.68 g (2.6 mmol) of scandium trichloride hexahydrate dissolved in 10 ml of 50% aqueous ethanol was added. The reaction mixture immediately became cloudy and a yellow oil slowly separated. After stirring for 2 hr, 100 ml of ethyl ether was added, and the precipitated sodium chloride was filtered off. The filtrate was dried over Drierite and the solvent was removed under reduced pressure at room temperature. The resulting yellow oil was vacuum distilled (Kugelrohr) at 240° (0.05 mm) and the product was obtained as a light yellow oil. *Anal.* Calcd for  $C_{39}H_{45}O_6Sc$ : C, 71.54; H, 6.93. Found: C, 71.44; H, 7.23.

**Tris(3-acetylpentane-2,4-dionato)aluminum(III) and -gallium(III), M(triac)<sub>3</sub>.**—These complexes were prepared from the tris(isopropoxides) and triacetylmethane<sup>33</sup> using the procedure for the corresponding pmhd complexes. Al(triac)<sub>3</sub> was recrystallized from benzene–heptane; white solid, mp 176–177°,  $\nu_{COCH_3}$  1675  $cm^{-1}$  (mull). *Anal.* Calcd for  $C_{21}H_{27}O_6Al$ : C, 55.99; H, 6.04. Found: C, 56.24; H, 6.08. Ga(triac)<sub>3</sub> was recrystallized five times from carbon tetrachloride; white solid, mp 175–189°,  $\nu_{COCH_3}$  1675  $cm^{-1}$  (mull). *Anal.* Calcd for  $C_{21}H_{27}O_6Ga$ : C, 51.15; H, 5.52. Found: C, 51.35; H, 5.51.

**Tris(3-acetylpentane-2,4-dionato)scandium(III), Sc(triac)<sub>3</sub>.**—Sc(acac)<sub>3</sub> was dissolved in a 4–5-fold excess of triacetylmethane and the volatile materials were removed at a diffusion pump. The process was repeated and the yellowish residue was recrystallized from chloroform–hexane and then from ether–hexane to give the somewhat impure complex as yellow crystals, mp 160–162°;  $\nu_{COCH_3}$  1675  $cm^{-1}$ . *Anal.* Calcd for  $C_{21}H_{27}O_6Sc$ : C, 53.84; H, 5.81. Found: C, 54.51; H, 5.29.

The stretching frequencies of the uncoordinated keto group correspond closely to those observed for other triac complexes.<sup>34</sup> The only triac complex of aluminum, gallium, or scandium which has been prepared previously is Al(triac)<sub>2</sub>(acac).<sup>34b</sup>

Al(acac)<sub>3</sub>, Ga(acac)<sub>3</sub>, and Sc(acac)<sub>3</sub> were prepared and purified by standard methods.

**Pmr Spectra.**—These spectra were recorded on a Varian HA-100 spectrometer equipped with a variable-temperature probe. Sample temperatures were measured with a thermocouple mounted in the probe. The thermocouple was calibrated by measuring the probe temperature in the standard way with either methanol or ethylene glycol using the frequency difference vs. temperature data of Van Geet.<sup>35</sup> Temperatures are considered accurate to  $\pm 1^\circ$  and variation at a given temperature was less than  $\pm 0.1^\circ$ . Duplicate spectra, recorded in opposite directions, were superposable and chemical shifts of resolved peaks are believed accurate to  $\pm 0.1$  Hz. All chemical shifts were referred to TMS as an internal reference. The complete

range of spectra of a given compound was recorded at a single continuous session on the nmr spectrometer in order to minimize the effects of any day to day irreproducibility. The concentration of solutions employed in measurements over a temperature range was ca. 0.4 M at 25°. Chlorobenzene was purified by the procedure described elsewhere.<sup>1</sup>

**Analysis of the Pmr Spectra.**—The spectra of Al(pmhd)<sub>3</sub> and Ga(pmhd)<sub>3</sub> in chlorobenzene solution were studied as a function of temperature. The slow-exchange limit was easily obtained for both and the fast-exchange limit was reached for the gallium complex. This limit was very closely approached for the aluminum complex. Rearrangement reactions were shown to be intramolecular by the observation of certain mixed-ligand complexes, as described in the text. Mechanisms of these reactions were investigated by calculations of line shapes in the intermediate-exchange regions for the various twist and bond rupture processes described in detail in part I.<sup>1</sup> The Whitesides–Lisle EXCNMR computer program,<sup>36</sup> based on the methods of Kubo and Sack,<sup>37</sup> was employed with minor modifications. Input data for this program consist of the chemical shifts, line widths, relative intensities of each of the pmr lines in the absence of exchange, and the kinetic exchange matrix. The program computes a line shape at specified values of the preexchange lifetime  $\tau$  of the trans isomer and plots this line shape on a Cal-comp plotter. The various mechanisms are specified by different exchange matrices, the nondiagonal elements of which are the probability of exchange between the nonequivalent sites. The diagonal elements are defined such that each row of the matrix sums to zero. In the slow-exchange limit the methyl region of both complexes consists of eight spin doublets produced by coupling of the methine proton with magnetically inequivalent methyl groups of each  $\gamma$ -*i*-C<sub>3</sub>H<sub>7</sub> substituent in the cis and trans forms. The coupling constants  $J_{H-CH_3}$  for all such doublets were found to be  $6.9 \pm 0.1$  Hz in *cis*- and *trans*-Al(pmhd)<sub>3</sub>, -Ga(pmhd)<sub>3</sub>, and -Co(pmhd)<sub>3</sub>. The same value was obtained in the fast-exchange region of the first two complexes and of Sc(pmhd)<sub>3</sub>. In order to conserve computer time the theoretical line shape was calculated for only the downfield component of each of the eight doublets. The program EXCNMR was modified in such a manner that the line shape plotted as output was a superposition of the calculated line shape for the downfield components and an identical line shape displaced by 6.9 Hz for the upfield components. The area of the upfield component was weighted to be 0.89 times that of the downfield component. This weighting factor was empirically determined from the ratios of the two components of the isopropyl methyl doublet in the spectrum of H(pmhd) and in the fast-exchange spectra of Al(pmhd)<sub>3</sub>, Ga(pmhd)<sub>3</sub>, and Sc(pmhd)<sub>3</sub>. The difference in intensity for the two components arises from second-order spin coupling effects. The upfield components of the isopropyl methine septet are more intense than the downfield components. Methyl line widths of the aluminum and gallium complexes were temperature independent in the ranges 25–85 and 30–40°, respectively, but increased at lower temperatures in the slow-exchange regions of both complexes. The same effect has been noticed for other  $\beta$ -diketonate complexes.<sup>23,38</sup> Line widths in the absence of exchange were obtained from a combination of measurements of experimental spectra in these ranges and the best fits of these to computed spectra for different line widths. The values of 0.7 and 0.8 Hz were adopted for all methyl signals of Al(pmhd)<sub>3</sub> and Ga(pmhd)<sub>3</sub>, respectively. The same value for Ga(pmhd)<sub>3</sub> was found in the fast-exchange limit. Values of chemical shifts employed in the slow- and intermediate-exchange regions, assignments of signals in slow-exchange regions, and evaluation of the cis:trans ratios at temperatures above this region are discussed in the text. The possible mechanisms were evaluated by visual comparison of computed and experimental isopropyl methyl spectra in the intermediate-exchange region.

## Results and Discussion

**Pmr Spectra. (a)  $\beta$ -H Region.**—Chemical shifts of the  $\beta$ -H and  $\gamma$ -*i*-C<sub>3</sub>H<sub>7</sub> methyl signals of M(pmhd)<sub>3</sub> complexes (M = Al, Ga, Co) in chlorobenzene solution at 29° (slow-exchange conditions) are listed in Table I.

(36) G. M. Whitesides and J. S. Fleming, *J. Amer. Chem. Soc.*, **89**, 2855 (1967); J. B. Lisle, S.B. Thesis, M.I.T., 1968.

(37) R. Kubo, *Nuovo Cimento, Suppl.*, **6**, 1063 (1957); R. A. Sack, *Mol. Phys.*, **1**, 163 (1958).

(38) R. C. Fay and R. N. Lowry, *Inorg. Chem.*, **6**, 1512 (1967).

(31) R. C. Mehrotra and R. K. Mehrotra, *Curr. Sci.*, **33**, 241 (1964).

(32) E. W. Berg and J. J. C. Acosta, *Anal. Chim. Acta*, **40**, 101 (1968).

(33) H. Paul, *J. Prakt. Chem.*, **21**, 186 (1963).

(34) (a) J. P. Collman, R. L. Marshall, W. L. Young, III, and C. T. Sears, Jr., *J. Org. Chem.*, **28**, 1449 (1963); (b) P. C. Doolan and P. H. Gore, *J. Chem. Soc. C*, 211 (1967).

(35) A. L. Van Geet, *Anal. Chem.*, **40**, 2227 (1968).

TABLE I  
PMR DATA FOR  $M(\text{pmhd})_3$  COMPLEXES IN  
CHLORO BENZENE SOLUTION AT 29°

Peak	Chem shifts, <sup>a</sup> Hz			
	<i>cis</i> - Co(pmhd) <sub>3</sub>	<i>trans</i> - Co(pmhd) <sub>3</sub>	Al(pmhd) <sub>3</sub>	Ga(pmhd) <sub>3</sub>
$\text{CH}_3(\gamma\text{-}i\text{-C}_3\text{H}_7)^b$	T <sub>1</sub>	-83.1	-82.7	-82.9
	C <sub>1</sub>	-86.1	-85.2	-85.7
	T <sub>2</sub>		-93.5	-90.8
	T <sub>3</sub>		-93.5	-92.7
	T <sub>4</sub>		-94.8	-93.6
	C <sub>2</sub>	-97.3	-96.1	-96.1
	T <sub>6</sub>		-101.7	-97.6
$\beta\text{-H}$	T	-544.6	-538.0	-531.7
	C	-546.5	-540.0	-534.5
	T		-546.5	-541.0
	T		-548.4	-542.8

<sup>a</sup> At 100 MHz, TMS internal reference. <sup>b</sup> Shifts of centers of spin doublets are given;  $J = 6.9 \pm 0.1$  Hz for all complexes.

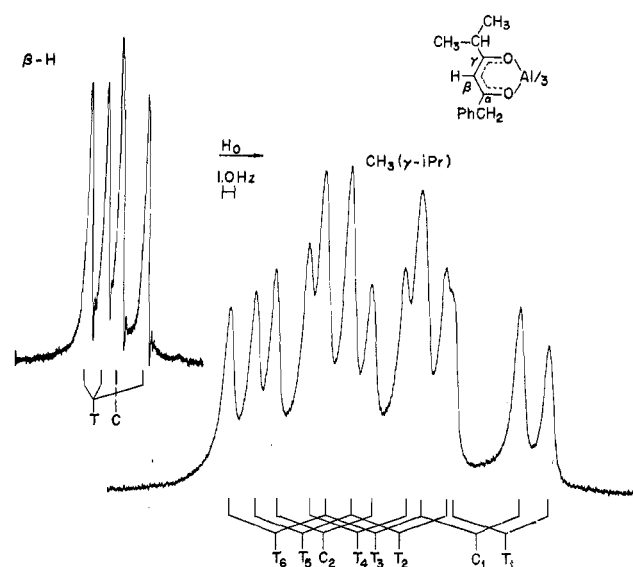


Figure 2.—The 100-MHz pmr spectrum of a mixture of *cis* (C) and *trans* (T) isomers of  $\text{Al}(\text{pmhd})_3$  in chlorobenzene solution at *ca.* 29° in the  $\beta\text{-H}$  and  $\gamma\text{-}i\text{-C}_3\text{H}_7$  methyl regions. The designations T<sub>1</sub>, C<sub>1</sub>, etc., refer to the centers of methyl spin doublets, whose chemical shifts at this temperature are given in Table I.

A sample spectrum of  $\text{Al}(\text{pmhd})_3$  is illustrated in Figure 2. The  $\beta\text{-H}$  region consists of four signals, three of which arise from the *trans* (C<sub>1</sub>) isomer and one from the *cis* (C<sub>3</sub>) isomer. The relative intensities of these signals show that the *cis* form is present in more than the 25 mol % expected for a purely statistical isomer distribution. Mole fractions of *cis*- $\text{Al}(\text{pmhd})_3$  and  $\text{-Ga}(\text{pmhd})_3$  were estimated at a series of temperatures in the slow-exchange region by a least-squares fitting of four Lorentzian lines to the observed  $\beta\text{-H}$  spectra. From this procedure thermodynamic data for the *cis*  $\rightleftharpoons$  *trans* equilibria of these complexes were obtained and are set out in Table II. The very small enthalpy changes are consistent with those found for the isomerization of several  $\text{M}(\text{tfac})_3$  complexes<sup>13</sup> and  $\text{Ga}(\text{acac})_3\text{-Ga}(\text{dbm})_3$  ligand exchange.<sup>22</sup> As shown in Figures 3 and 4, the  $\beta\text{-H}$  signals of  $\text{Al}(\text{pmhd})_3$  and  $\text{Ga}(\text{pmhd})_3$  are markedly temperature dependent and coalesce to single broad features at *ca.* 125 and 75°, respectively. These signals sharpen at higher temperatures. This behavior is clearly indicative of a fast interconversion of *cis* and *trans* isomers. In the slow-exchange region (below *ca.*

TABLE II  
THERMODYNAMIC DATA FOR THE *CIS*  $\rightleftharpoons$  *TRANS* EQUILIBRIA  
OF  $\text{M}(\text{pmhd})_3$  COMPLEXES IN CHLORO BENZENE SOLUTION

Complex	$\Delta H^\circ$ , <sup>a</sup>	$\Delta S^\circ$ , <sup>a</sup>	$\Delta G^\circ_{298}$ , <sup>b</sup>	$K_{\text{eq}^{298}}$ , <sup>b</sup>
	kcal/mol	eu	kcal/mol	
$\text{Al}(\text{pmhd})_3$	$0.15 \pm 0.50$	$2.3 \pm 1.5$	$-0.55 \pm 0.07$	$2.5 \pm 0.3$
$\text{Ga}(\text{pmhd})_3$	$0.38 \pm 0.50$	$3.1 \pm 1.5$	$-0.54 \pm 0.07$	$2.5 \pm 0.3$

<sup>a</sup> Errors were estimated graphically from maximum and minimum slopes. Standard deviations calculated from scatter of experimental points:  $\text{Al}(\text{pmhd})_3$ ,  $\sigma(\Delta H^\circ) = 0.07$  kcal/mol,  $\sigma(\Delta S^\circ) = 0.2$  eu;  $\text{Ga}(\text{pmhd})_3$ ,  $\sigma(\Delta H^\circ) = 0.12$  kcal/mol,  $\sigma(\Delta S^\circ) = 0.4$  eu. <sup>b</sup> Estimated maximum errors.

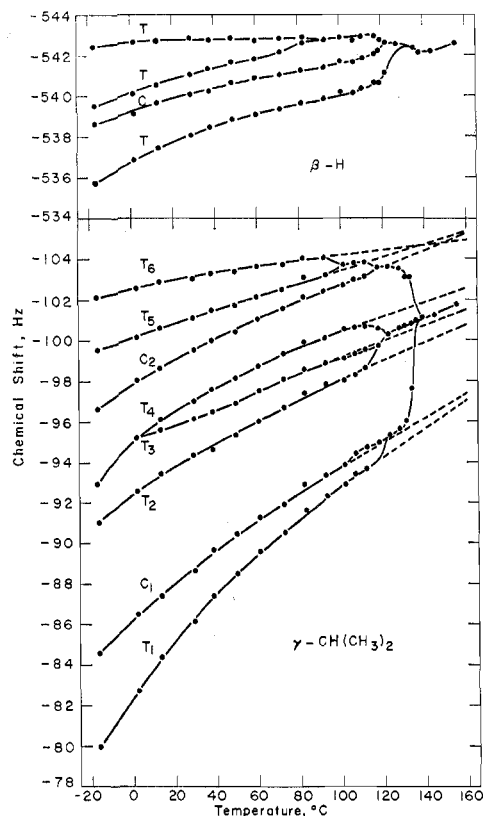


Figure 3.—Temperature dependencies of the chemical shifts of the  $\beta\text{-H}$  and  $\gamma\text{-}i\text{-C}_3\text{H}_7$  methyl signals of *cis* (C) and *trans* (T) isomers of  $\text{Al}(\text{pmhd})_3$  in chlorobenzene solution. The shifts of the low-field component of each methyl spin doublet are plotted.

80° for  $\text{Al}(\text{pmhd})_3$  and *ca.* 50° for  $\text{Ga}(\text{pmhd})_3$  the  $\beta\text{-H}$  shifts of both complexes exhibit a definite temperature dependence, which is also found for the isopropyl methyl resonances (*vide infra*).

(b) **Isopropyl Methyl Region.**—Under slow-exchange conditions signals in this region are more complex than are  $\beta\text{-H}$  resonances because they arise from magnetic inequivalence due to both geometrical and optical isomerism and spin coupling of the inequivalent methyl groups with the methine proton. The diastereotopic nature of the methyl groups in type 2 complexes is dramatically illustrated by the spectrum of pure *cis*- $\text{Co}(\text{pmhd})_3$ . The methyl region consists of two spin-spin doublets whose centers are separated by 11.2 Hz (*cf.* Table I). In *cis*-*trans* mixtures of pmhd complexes, the diastereotopic effect together with the four positionally inequivalent isopropyl environments leads to eight spin-spin doublets. Spectra of the methine region indicate that  $J_{\text{H-CH}_3}$  is the same ( $6.9 \pm 0.1$  Hz) for all such spin doublets of the cobalt, aluminum, and gallium complexes, thereby allowing pairing of the components

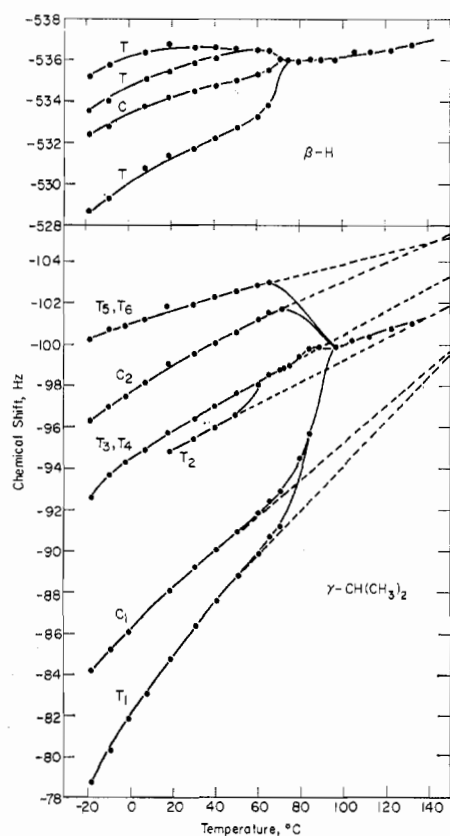


Figure 4.—Temperature dependencies of the chemical shifts of the  $\beta$ -H and  $\gamma$ -*i*-C<sub>3</sub>H<sub>7</sub> methyl signals of cis (C) and trans (T) isomers of Ga(pmhd)<sub>3</sub> in chlorobenzene solution. The shifts of the low-field component of each methyl spin doublet are plotted.

of each doublet of these complexes. Doublets arising from the cis isomers of Al(pmhd)<sub>3</sub> and Ga(pmhd)<sub>3</sub> were identified by their relative intensities and by comparison with the spectra of the separated cis and trans isomers of Co(pmhd)<sub>3</sub>. Assignments of doublet components, which are numbered sequentially from high to low field, are shown for Al(pmhd)<sub>3</sub> in Figure 2; chemical shifts of the centers of these doublets of the aluminum, gallium, and cobalt complexes are given in Table I.<sup>39</sup> In no case was spin coupling between magnetically inequivalent methyls of the same isopropyl group detectable. Temperature dependencies of methyl chemical shifts are shown in Figures 3 and 4; approximate temperatures at which coalescence to a single signal occurs are 140 and 85° for Al(pmhd)<sub>3</sub> and Ga(pmhd)<sub>3</sub>, respectively.

In order to carry out a line shape analysis in the intermediate-exchange regions of the aluminum and gallium complexes, assignments of the eight methyl spin doublets to specific magnetic environments at slow exchange are required. The environments are designated as T<sub>xr</sub>, T<sub>xs</sub>, T<sub>yr</sub>, T<sub>ys</sub>, T<sub>zr</sub>, T<sub>zs</sub>, C<sub>r</sub>, and C<sub>s</sub>, in which x, y, and z denote the three nonequivalent chelate rings of

(39) The methylene protons of the  $\alpha$ -benzyl group in **2** can in principle show chemical shift effects similar to those observed for the isopropyl methyls under slow-exchange conditions. However, their chemical shift spread is too small to be of value. The particular advantages of M(pmhd)<sub>3</sub> species are clearly the resolution in the methyl region at slow exchange and the detailed line shape changes under intermediate-exchange conditions. These features were not as well developed in a number of other tris( $\beta$ -diketonato)aluminum(III) complexes examined. For example, Al(mhd)<sub>3</sub> at 30° (slow exchange) shows only five resolvable isopropyl methyl signals with a chemical shift spread of 0.14 ppm in chlorobenzene.

the trans isomer defined in Figure 1, and r and s signify the different environments of the diastereotopic methyls of a given isopropyl group. A methyl group which is r in the  $\Delta$  configuration is s in the  $\Lambda$  configuration. The problem of making these assignments has been carried out in three stages: division of the six trans doublets (T<sub>1</sub>–T<sub>6</sub>) into three diastereotopic pairs; assignment of x, y, and z environments to these pairs; assignment of r and s environments within each of these three pairs and the cis pair C<sub>1</sub>, C<sub>2</sub>. There are 15 possible pairing schemes, 6 x, y, z assignment schemes, and 8 r, s assignment schemes,<sup>40</sup> leading to a total of 720 different ways to assign the doublets C<sub>1</sub>, C<sub>2</sub>, T<sub>1</sub>–T<sub>6</sub> to the environments C<sub>r</sub>, C<sub>s</sub>, T<sub>xr</sub>, . . . , T<sub>zs</sub>. This number has been reduced to manageable values by arguments based upon solvent and temperature dependencies of chemical shifts and nearest-neighbor environment effects.

Plots of chemical shift vs. temperature for the low-field components of the eight methyl spin doublets of Al(pmhd)<sub>3</sub> in chlorobenzene and chloroform solutions are shown in Figures 3 and 5, respectively. Line width

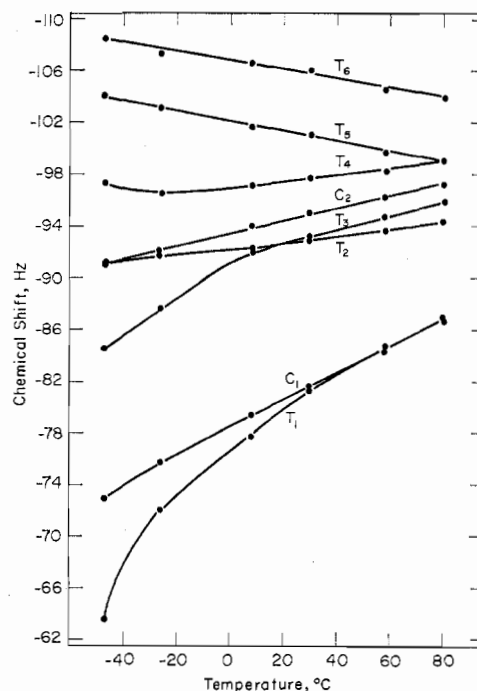


Figure 5.—Temperature dependencies of the  $\gamma$ -*i*-C<sub>3</sub>H<sub>7</sub> methyl chemical shifts of Al(pmhd)<sub>3</sub> in chloroform solution. The shifts of the low-field component of each methyl spin doublet are plotted.

measurements show that below *ca.* 85° the slow-exchange condition exists in both solvents. However, under this condition the chemical shifts are markedly temperature dependent. The shifts of the slow complex Co(pmhd)<sub>3</sub> in these two solvents manifest a very similar variation with temperature. Temperature-dependent shifts have also been observed in the slow-exchange <sup>19</sup>F<sup>7</sup> and <sup>1</sup>H<sup>23</sup> spectra of tris( $\beta$ -diketonates) of aluminum, gallium, and cobalt and in all cases are presumably due to changes in solvation with temperature.

(40) An absolute stereochemical definition of r and s is not given since the only significant fact is that upon inversion of configuration r goes into s and vice versa. Only the relative assignment of r and s between different diastereotopic pairs is detectable and interchange of all r's and s's produces an equivalent assignment scheme.

The chemical shift differences between the two *cis* doublets of  $\text{Al}(\text{pmhd})_3$  and  $\text{Co}(\text{pmhd})_3$  change only slightly with temperature in the two solvents or with solvent composition at constant temperature (cf. Figure 6).

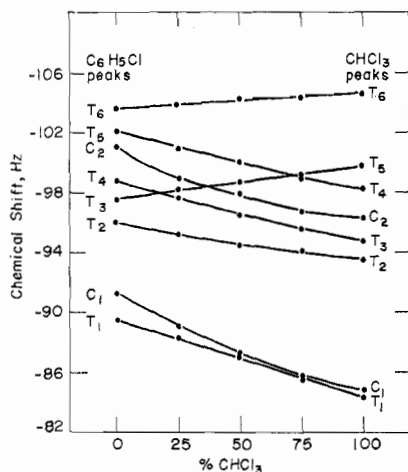
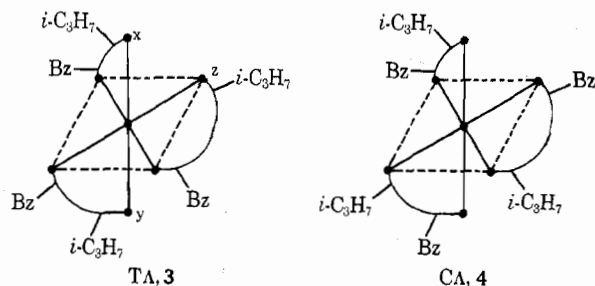


Figure 6.—Correlation of the  $\gamma$ - $i$ - $\text{C}_3\text{H}_7$  methyl chemical shifts of  $\text{Al}(\text{pmhd})_3$  in chloroform and chlorobenzene at  $59^\circ$ . The shifts of the low-field component of each methyl spin doublet are plotted as a function of volume per cent of chloroform. *Cis* and *trans* signals in the pure solvents are numbered from high to low field.

This implies that the components of a diastereotopic pair of signals show parallel chemical shift behavior in chloroform and chlorobenzene or in a mixture of the two solvents. Applying this criterion to the data in chloroform (Figure 5), where the chemical shift patterns are somewhat more distinctive than in chlorobenzene, it appears that the *trans* doublets should be placed in diastereotopic pairs as follows:  $T_1$ - $T_3$ ,  $T_2$ - $T_4$ ,  $T_5$ - $T_6$ . The pairing scheme in chlorobenzene solution has been obtained from shift measurements in mixed solvents which are summarized in Figure 6. The data in this figure correlate  $T_3$ ,  $T_4$ ,  $T_5$  in chloroform with  $T_4$ ,  $T_5$ ,  $T_3$  in chlorobenzene. The resultant pairing scheme in chlorobenzene,  $T_1$ - $T_4$ ,  $T_2$ - $T_5$ ,  $T_3$ - $T_6$ , is also consistent with the temperature dependencies of the chemical shifts, although the differences between the three pairs are not as clear-cut as they are in chloroform.

The magnetic environment of a given isopropyl group in the *trans* (3) and *cis* (4) isomers should be largely determined by its nearest neighbors. In particular, space-filling molecular models show that the isopropyl methyls are approached rather closely by the phenyl rings of benzyl (Bz) groups on adjacent ligands.



For the three inequivalent isopropyl groups of the *trans* isomer the nearest substituents are the following: (x) Bz, Bz,  $i$ - $\text{C}_3\text{H}_7$ ; (y) Bz,  $i$ - $\text{C}_3\text{H}_7$ , Bz; (z)  $i$ - $\text{C}_3\text{H}_7$ , Bz,

$i$ - $\text{C}_3\text{H}_7$ . For the three equivalent isopropyl groups of the *cis* isomer these substituents are  $i$ - $\text{C}_3\text{H}_7$ ,  $i$ - $\text{C}_3\text{H}_7$ , Bz. It is therefore expected that groups x and y in the *trans* isomer will show similar chemical shifts and that the *trans*-z and *cis* isomers will do likewise. In general, the pmr spectra of alkyl ring substituents in *trans*-tris( $\beta$ -diketonates) at slow exchange<sup>1,12,13,15</sup> consist of two resonances relatively close together and a third upfield of these two. The *cis* resonance falls between these two groups, usually nearer the upfield signal. For example, the 100-MHz spectrum of the methyl group in tris-(1-phenylpentane-2,4-dionato)aluminum(III) contains signals at  $-157.5$  (*cis* + *trans*),  $-166.3$  (*trans*), and  $-169.9$  Hz (*trans*). The last two resonances are assigned to x and y environments and the upfield resonance is assigned to the z environment. Using this approach the pair  $T_1$ - $T_4$  of  $\text{Al}(\text{pmhd})_3$  is assigned to the z environment and the pairs  $T_2$ - $T_5$ ,  $T_3$ - $T_6$  are assigned to the x, y environments. This assignment makes the *trans*-z diastereotopic splitting approximately the same as that of  $C_1$ - $C_2$ , which is considered reasonable if the methyl groups are indeed in similar magnetic environments. The pairs  $T_2$ - $T_5$  and  $T_3$ - $T_6$  cannot be assigned specifically to the x or y environments.

The slow-exchange spectrum of  $\text{Ga}(\text{pmhd})_3$  in chlorobenzene is rather similar to that of  $\text{Al}(\text{pmhd})_3$  but differs in that the spin doublets  $T_3$ - $T_4$  and  $T_5$ - $T_6$  coincide in chemical shift (cf. Figure 4). On the basis of experimental observations and arguments analogous to those used in the aluminum case, pairing schemes of the six *trans* doublets and assignments of pairs of doublets to x, y, z environments have been deduced. However, it was not possible to determine uniquely whether the z resonances should be  $T_1$ - $T_2$  or  $T_1$ - $T_3$ . Assignments of  $T_1$ - $T_6$  doublets for the two complexes in chlorobenzene are summarized below.<sup>41</sup> Each of the assignments of three pairs of *trans* doublets to x, y, z environments has

	Al(pmhd) <sub>3</sub>		Ga(pmhd) <sub>3</sub>		
	A	B	C	D	E
x	$T_2$ - $T_5$	$T_3$ - $T_6$	$T_3$ - $T_5$	$T_2$ - $T_5$	$T_4$ - $T_3$
y	$T_3$ - $T_6$	$T_2$ - $T_5$	$T_4$ - $T_6$	$T_4$ - $T_6$	$T_2$ - $T_5$
z	$T_1$ - $T_4$	$T_1$ - $T_4$	$T_1$ - $T_2$	$T_1$ - $T_3$	$T_1$ - $T_3$

associated with it eight r, s assignments. No plausible arguments can be advanced to reduce the number of r, s assignments. By the procedure described the total of 720 possible overall assignments of methyl signals in a *cis*-*trans* mixture of  $\text{M}(\text{pmhd})_3$  complexes has been reduced to the following:  $\text{M} = \text{Al}$ , 2 (A, B)  $\times$  8 (r, s) = 16;  $\text{M} = \text{Ga}$ , 3 (C, D, E)  $\times$  8 (r, s) = 24. It is emphasized that the assignments set out above are not subject to any unequivocal proof. However, they are fully consistent with all experimental observations and are thus considered the most probable.

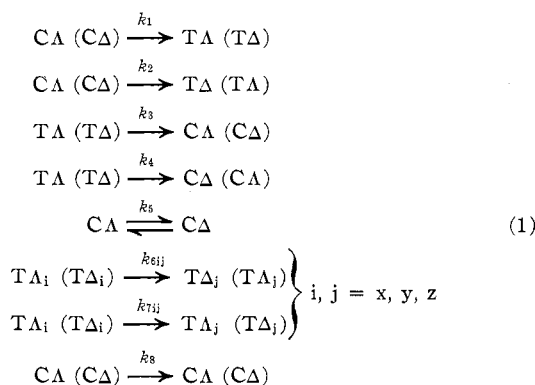
**Evidence for the Intramolecular Nature of the Rearrangements.**—Equilibration of chlorobenzene solutions containing  $\text{M}(\text{acac})_3$  and  $\text{M}(\text{pmhd})_3$  results in the formation of mixed-ligand complexes  $\text{M}(\text{acac})_{3-n}(\text{pmhd})_n$ . The formation of mixed species is slow compared to the rate of intramolecular rearrangement. No pmr signals attributable to mixed complexes could be detected in a 1:3 mixture of  $\text{Al}(\text{acac})_3$ - $\text{Al}(\text{pmhd})_3$  after

(41) Because of the equal chemical shifts of  $T_3$  and  $T_4$  and of  $T_5$  and  $T_6$ , a number of other representations of the three different assignment schemes for  $\text{Ga}(\text{pmhd})_3$  are possible. However, in terms of pmr spectral differences these are either identical with or equivalent to the assignments given above.



1 hr at room temperature. Equilibration was accomplished by heating the sample at  $\sim 80^\circ$  for several hours. The gallium complexes are faster and exchange appears to be complete within 10–15 min after mixing at room temperature. Pmr spectra of the equilibrium mixtures indicate that ligand exchange is slow compared to the rate of environmental averaging. At temperatures where the  $\beta$ -H and isopropyl methyl signals of pure  $\text{Al}(\text{pmhd})_3$  are averaged, multiple signals are observed in the mixture. For example, 10 of the 15  $\beta$ -H signals possible for a solution containing the two pure- and mixed-ligand complexes are resolved at  $30^\circ$ . At  $150^\circ$  three signals each for acac and pmhd  $\beta$ -H's are observed in the range  $-5.30$  to  $-5.48$  ppm, consistent with fast intramolecular rearrangement of species with  $n = 1, 2, 3$  and slow ligand exchange. Analogous observations were made for the gallium system at 30 and  $120^\circ$ . The results for the aluminum and gallium systems are consistent with the previously observed behavior of other mixed-ligand tris( $\beta$ -diketonato) complexes of these metal ions, for which slow ligand exchange under conditions of fast environmental averaging was found.<sup>8,23</sup>

**Treatment of Kinetics.**—Rearrangements of the four isomers  $\text{C}\Delta$ ,  $\text{C}\Lambda$ ,  $\text{T}\Delta$ , and  $\text{T}\Lambda$  are characterized by the eight microscopic rate constants for the transformations of (1). The rate constants  $k_{6ij}$  and  $k_{7ij}$  refer to



the transfer of a nucleus from environment  $i$  (trans) to environment  $j$  (trans) with and without inversion of the molecular configuration, respectively. The rate of conversion of trans  $\Lambda$  to trans  $\Delta$  is  $\sum_j k_{6ij}$  for any  $i$ . Of necessity  $k_{6ij} (k_{7ij}) = k_{6ji} (k_{7ji})$ . The rate constants  $k_{7ii}$  and  $k_8$ , which denote passage through a transition state to re-form the initial isomer, are included for completeness and because their values may differ from one mechanism to another.

The intramolecular processes by which intramolecular rearrangements can take place are of two types: those in which one bond is broken to form a five-coordinate transition state (idealized TBP or SP structure) and those in which all six metal–oxygen bonds remain intact throughout the rearrangement (twist mechanism with the idealized trigonal-prismatic transition state). These mechanisms have been treated in detail in part I<sup>1</sup> and will be discussed only briefly here. Rearrangements due to rupture of two bonds are neglected in the kinetic treatment because of the high activation energy required.<sup>7</sup> An important difference between the slow and fast cases is that in the latter scrambling of inequivalent ligand environments which

accompanies a trans-to-trans conversion is detectable by nmr. The six possible scrambling schemes are presented in Table III and in subsequent discussion will be

TABLE III  
SCRAMBLING PATTERNS OF ENVIRONMENTS  
x, y, z IN  $\text{T}\Lambda \rightarrow \text{T}\Delta$ ,  $\text{T}\Lambda$  REARRANGEMENTS

$\alpha$	$x \rightarrow x$	$\delta$	$x \rightarrow y$
	$y \rightarrow y$		$y \rightarrow x$
	$z \rightarrow z$		$z \rightarrow z$
$\beta$	$x \rightarrow x$	$\epsilon$	$x \rightarrow y$
	$y \rightarrow z$		$y \rightarrow z$
	$z \rightarrow y$		$z \rightarrow x$
$\gamma$	$x \rightarrow z$	$\mu$	$x \rightarrow z$
	$y \rightarrow y$		$y \rightarrow x$
	$z \rightarrow x$		$z \rightarrow y$

referred to by the designations in this table.

Rearrangements which occur without bond breaking may be most easily visualized as proceeding through twist motions of the ligands around axes bisecting opposite triangular faces of the coordination octahedron. Adopting the Springer–Sievers notation,<sup>8</sup> the axes are designated as real (r), pseudo (p), and imaginary (i)  $C_3$  axes. Certain of these axes in cis- $\Delta$  and trans- $\Lambda$  isomers are shown in Figure 1. Illustrative twists about the p- and one of the three inequivalent i- $C_3$  axes ( $i-C_3'$ ,  $-C_3''$ ,  $-C_3'''$ ) of trans- $\Lambda$  isomers are given in Figure 7. The notation of transition states in this and other rearrangement mechanisms is the same as that used elsewhere.<sup>1</sup> Transition states and products obtained by twists about all  $C_3$  axes are presented in Table IV. Because of the inequivalence of the i- $C_3$  axes of a

TABLE IV  
ISOMER DISTRIBUTIONS AND MICROSCOPIC  
RATE CONSTANTS FOR TWIST MECHANISMS

Initial isomer	Isomer Distributions		
	Rotation axis	Transition state <sup>a</sup>	Products
$\text{C}\Lambda$	r- $C_3$	1	$\text{C}\Delta + \text{C}\Lambda$
	i- $C_3$	2l	$\text{T}\Delta + \text{C}\Lambda$
	p- $C_3$	3	$\text{T}\Delta\beta + \text{T}\Lambda\alpha$
$\text{T}\Lambda$	i- $C_3'$	2d	$\text{C}\Delta + \text{T}\Lambda\alpha$
	i- $C_3''$	4l	$\text{T}\Delta\mu + \text{T}\Lambda\alpha$
	i- $C_3'''$	4d	$\text{T}\Delta\epsilon + \text{T}\Lambda\alpha$

Rate Constants <sup>b,c</sup>		
$\text{C}\Lambda \xrightarrow{k'} \text{C}\Delta + 3\text{T}\Delta + 4\text{C}\Lambda$	$\text{T}\Lambda \xrightarrow{k''} \text{C}\Delta + 3\text{T}\Delta\beta + \epsilon + \mu + 4\text{T}\Lambda\alpha$	
$k_1 = 0$	$k_{6xx} = R_p k''/2$	$k_{7xx} = k''/2$
$k_2 = (1 - R_r)k'/2$	$k_{6yy} = 0$	$k_{7yy} = k''/2$
$k_3 = 0$	$k_{6zz} = 0$	$k_{7zz} = k''/2$
$k_4 = (1 - R_p)k''/6$	$k_{6xy} = (1 - R_p)k''/6$	$k_{7xy} = 0$
$k_5 = R_r k'/2$	$k_{6xz} = (1 - R_p)k''/6$	$k_{7xz} = 0$
$k_8 = k'/2$	$k_{6yz} = (1 + 2R_p)k''/6$	$k_{7yz} = 0$
$K_{eq} = \frac{3(1 - R_r)k'}{(1 - R_p)k''} \quad k' = \frac{(1 - R_p)k''K_{eq}}{3(1 - R_r)}$		

<sup>a</sup> For specifications of transition states cf. Figures 5, 7, and 9 of ref 1. <sup>b</sup> Product distribution assuming rotations about all threefold axes equally probable. <sup>c</sup> Rotations about i- $C_3'$ , i- $C_3''$ , and i- $C_3'''$  treated as equally probable.

trans isomer, rates of rotation about them may be different. To reduce the extent of parameterization in the line shape calculations, rotations about these axes are assumed equally probable. The rate constants  $k_1$ – $k_8$  are given in Table IV as a function of the prob-

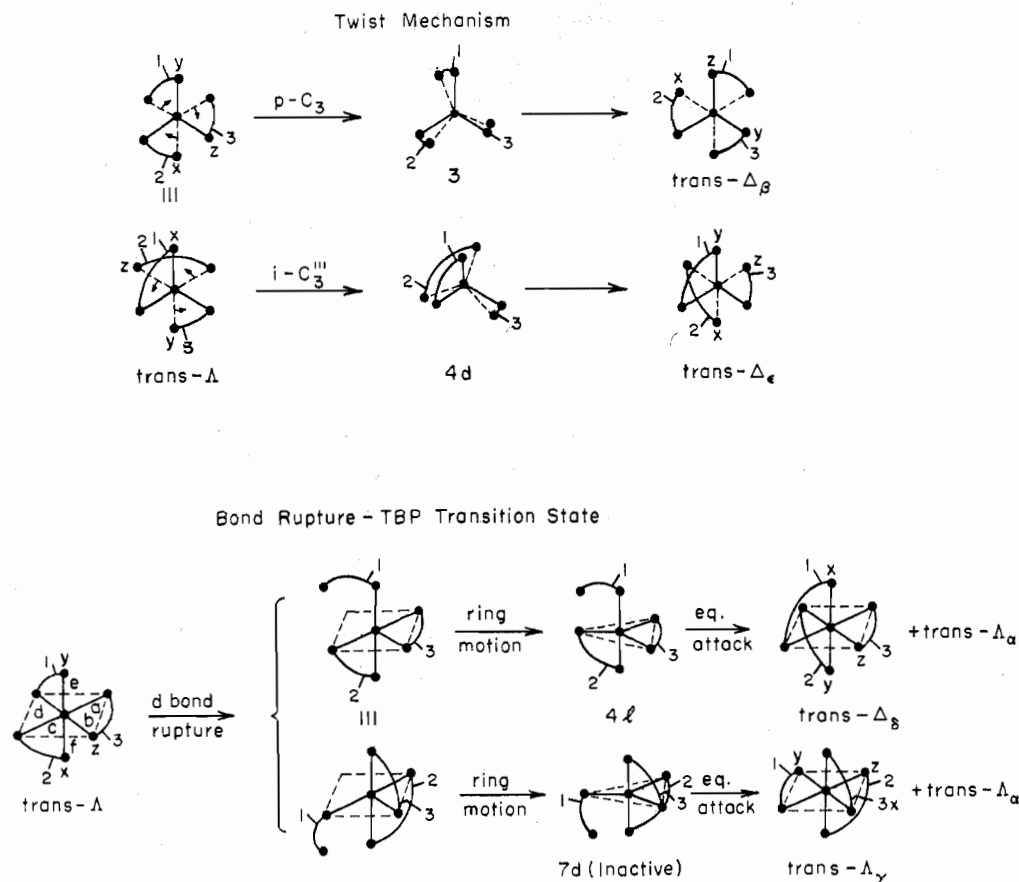


Figure 7.—Illustration of rearrangement reactions of the trans- $\Delta$  isomer proceeding by the twist and bond rupture mechanisms. TBP transition states 4l and 7d possess dangling axial and equatorial ligands, respectively. The scrambling schemes  $\alpha$ - $\epsilon$  are defined in Table III. Transition state 7d is inactive in racemization and isomerization but does lead to scrambling of ring substituents.

ability  $R$  of rotation about the  $r$ - and  $p$ - $C_3$  axes.<sup>42</sup> The rate constants  $k'$  and  $k''$  represent the rates of formations of transition states from cis and trans isomers, respectively, which may generate product or starting isomer. All twists occur exclusively with *inversion* of configuration.

Considering next bond rupture mechanisms, an illustrative process involving TBP transition states is shown in Figure 7. Breaking of one of the six inequivalent bonds in the trans- $\Delta$  isomer leads to the axial and equatorial transition states 4l and 7d, respectively. The transition states and products obtained by rupture of all inequivalent bonds in cis- and trans- $\Delta$  isomers and the rate constants  $k_1$ - $k_8$  for the TBP mechanism are set out in Table V. The rate constants are specified on the assumption that all bonds break with equal probability. Again,  $k'$  and  $k''$  are the rates of formation of transition states from cis and trans forms, which may give product or initial isomer. Rearrangement through a TBP-axial transition state always occurs with *inversion* of configuration whereas rearrangement through a TBP-equatorial transition state always occurs with *retention* of configuration.

An SP transition state with the dangling ligand occupying a basal position is kinetically equivalent to

(42)  $R_r + 3R_l = 1$  for cis isomers and  $R_p + R_l' + R_l'' + R_l''' = 1$  for trans isomers. The assumption that  $R_l' = R_l'' = R_l'''$  means that trigonal-prismatic transition states with two chelate rings attached to triangular faces and the third disposed along the edge of a rectangular face are equally probable. Rotation about  $r$ - and  $p$ - $C_3$  axes yields transition states in which all three ligands have the latter arrangement (*cf.* ref 10).

TABLE V  
ISOMER DISTRIBUTIONS AND MICROSCOPIC  
RATE CONSTANTS FOR TBP MECHANISMS

Initial isomer	Bond broken	Transition state <sup>a</sup>		Products	
		Axial	Eq	Axial	Eq
CA	a	3l	5d	T $\Delta$ + CA	TA + CA
	b	2d	6d	T $\Delta$ + CA	TA + CA
TA	a	3d	9d	CA + T $\Delta_\alpha$	T $\Delta_\delta$ + T $\Delta_\alpha$
	b	1d	10d	T $\Delta_\gamma$ + T $\Delta_\alpha$	T $\Delta_\delta$ + T $\Delta_\alpha$
	c	4d	5d	T $\Delta_\delta$ + T $\Delta_\alpha$	CA + T $\Delta_\alpha$
	d	4l	7d	T $\Delta_\delta$ + T $\Delta_\alpha$	T $\Delta_\gamma$ + T $\Delta_\alpha$
	e	2l	8d	CA + T $\Delta_\alpha$	T $\Delta_\gamma$ + T $\Delta_\alpha$
	f	1l	6d	T $\Delta_\gamma$ + T $\Delta_\alpha$	CA + T $\Delta_\alpha$

TBP-Axial Rate Constants

$$\begin{aligned}
 \text{CA} &\xrightarrow{k'} \text{T}\Delta + \text{CA}; \quad \text{TA} \xrightarrow{k''} \text{CA} + 2\text{T}\Delta_{\gamma+\delta} + 3\text{T}\Delta_\alpha \\
 k_1 &= 0 & k_{6xx} &= 0 & k_{7xx} &= k''/2 \\
 k_2 &= k'/2 & k_{6yy} &= k''/6 & k_{7yy} &= k''/2 \\
 k_3 &= 0 & k_{6zz} &= k''/6 & k_{7zz} &= k''/2 \\
 k_4 &= k''/6 & k_{6xy} &= k''/6 & k_{7xy} &= 0 \\
 k_5 &= 0 & k_{6xz} &= k''/6 & k_{7xz} &= 0 \\
 k_6 &= k'/2 & k_{6yz} &= 0 & k_{7yz} &= 0
 \end{aligned}$$

TBP-Equatorial Rate Constants

$$\begin{aligned}
 \text{CA} &\xrightarrow{k'} \text{TA} + \text{CA}; \quad \text{TA} \xrightarrow{k''} \text{CA} + 2\text{T}\Delta_{\gamma+\delta} + 3\text{T}\Delta_\alpha \\
 k_1 &= k'/2 & k_{7xx} &= k''/2 \\
 k_2 &= 0 & k_{7yy} &= 2k''/3 \\
 k_3 &= k''/6 & k_{7zz} &= 2k''/3 \\
 k_4 &= 0 & k_{7xy} &= k''/6 \\
 k_5 &= 0 & k_{7xz} &= k''/6 \\
 k_{6ij} &= 0 & k_{7yz} &= 0 \\
 k_8 &= k'/2
 \end{aligned}$$

TBP-axial and eq:  $K_{eq} = 3k'/k''$ ;  $k' = k''K_{eq}/3$

<sup>a</sup> For specification of transition states *cf.* Figures 5, 7, and 9 of ref 1.



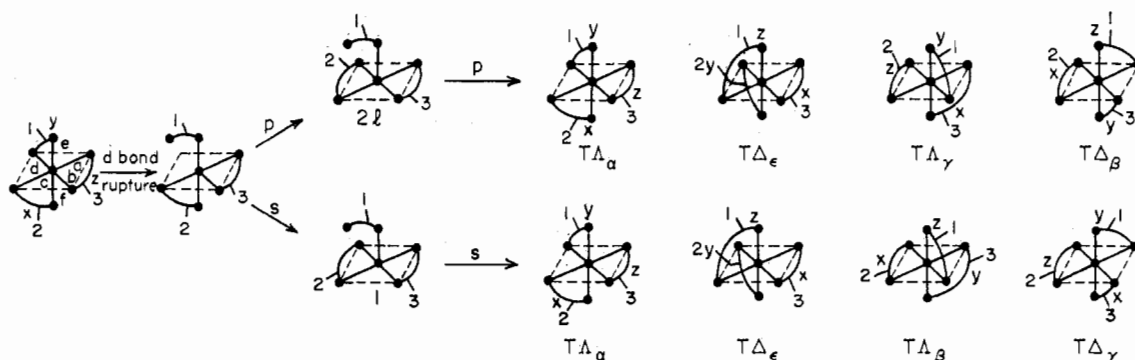


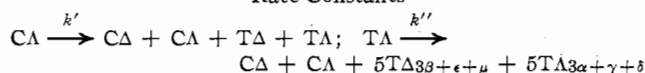
Figure 8.—Illustration of the rearrangement reactions of the trans- $\Delta$  isomer proceeding through SP-axial transition states formed by rupture of bond d. Note that 2l and 1 can pass to products by both primary (p) and secondary (s) processes, only half of which are shown (cf. Table VII). The scrambling schemes  $\alpha$ - $\epsilon$  are defined in Table III.

a TBP-axial transition state.<sup>1</sup> Rearrangement *via* SP-axial transition states is complicated by the possibility of two microscopically reversible pathways for formation of transition states and products. These pathways, designated as primary (p) and secondary (s),<sup>1</sup> are illustrated in Figure 8, which shows the transition states and half of the products arising from the rupture of one bond in the trans- $\Delta$  isomer. In the example given the difference between the two processes is in the motion of ligand 2 after rupture of bond d. Two transition states, 2l and 1, are formed and each may pass to products by both primary and secondary processes. On the basis of earlier considerations,<sup>1</sup> rearrangements involving SP-axial transition states will most likely involve the primary process alone or a 1:1 mixture of primary and secondary processes. Listed in Tables VI and VII are transition states, product dis-

TABLE VI  
ISOMER DISTRIBUTIONS AND MICROSCOPIC  
RATE CONSTANTS FOR THE SP-PRIMARY MECHANISM

Isomer Distributions			
Initial isomer	Bond broken	Transition state <sup>a</sup>	Products
CA	a	1	CA + T $\Delta$ + T $\Lambda$ + CA
	b	3	T $\Lambda$ + CA + CA + T $\Delta$
TA	a	2d	T $\Lambda_\alpha$ + T $\Delta_\mu$ + T $\Lambda_\delta$ + T $\Delta_\beta$
	b	4d	T $\Lambda_\delta$ + T $\Delta_\beta$ + T $\Lambda_\alpha$ + T $\Delta_\mu$
	c	1	T $\Lambda_\alpha$ + CA + CA + T $\Delta_\beta$
	d	2l	T $\Lambda_\alpha$ + T $\Delta_\epsilon$ + T $\Lambda_\gamma$ + T $\Delta_\beta$
	e	4l	T $\Lambda_\gamma$ + T $\Delta_\beta$ + T $\Lambda_\alpha$ + T $\Delta_\epsilon$
	f	3	CA + T $\Delta_\beta$ + T $\Lambda_\alpha$ + CA

#### Rate Constants



$$\begin{array}{lll} k_1 = k'/4 & k_{\delta_{xx}} = k''/4 & k_{\tau_{xx}} = k''/4 \\ k_2 = k'/4 & k_{\delta_{yy}} = 0 & k_{\tau_{yy}} = k''/3 \\ k_3 = k''/12 & k_{\delta_{zz}} = 0 & k_{\tau_{zz}} = k''/3 \\ k_4 = k''/12 & k_{\delta_{xy}} = k''/12 & k_{\tau_{xy}} = k''/12 \\ k_5 = k'/4 & k_{\delta_{xz}} = k''/12 & k_{\tau_{xz}} = k''/12 \\ k_6 = k'/4 & k_{\delta_{yz}} = k''/3 & k_{\tau_{yz}} = 0 \end{array}$$

$$K_{eq} = 3k'/k''; \quad k' = k''K_{eq}/3$$

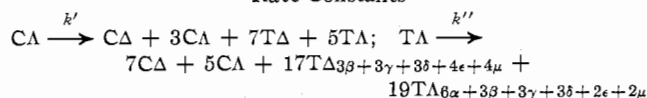
<sup>a</sup> For specification of transition states cf. Figures 5, 7, and 9 of ref 1.

tributions, and rate constants for the two cases. It is assumed that inequivalent bonds in cis and trans isomers break with equal probability and that in each transition state the four corners of the basal plane are

TABLE VII  
ISOMER DISTRIBUTIONS AND MICROSCOPIC RATE CONSTANTS FOR  
THE SP 50% PRIMARY-50% SECONDARY MECHANISM

Isomer Distributions				
Initial isomer	Bond broken	Transition states <sup>a</sup>		Products
		Primary	Secondary	
CA	a	1	2l	CA + 3CA + 7T $\Delta$ + 5T $\Lambda$
	b	3	4d	CA + 3CA + 7T $\Delta$ + 5T $\Lambda$
TA	a	2d	1	3CA + CA + T $\Delta_\beta$ + T $\Delta_\delta$ + T $\Delta_\epsilon$ + 2T $\Delta_\mu$ + 2T $\Lambda_\alpha$ + T $\Lambda_\beta$ + 2T $\Lambda_\gamma$ + T $\Lambda_\delta$ + T $\Lambda_\epsilon$
	b	4d	3	CA + 3CA + T $\Delta_\beta$ + 2T $\Delta_\gamma$ + T $\Delta_\delta$ + T $\Delta_\epsilon$ + 2T $\Delta_\mu$ + 2T $\Lambda_\alpha$ + T $\Lambda_\beta$ + T $\Lambda_\delta$ + T $\Lambda_\epsilon$
	c	1	2d	3CA + CA + T $\Delta_\beta$ + 2T $\Delta_\delta$ + T $\Delta_\epsilon$ + T $\Delta_\mu$ + 2T $\Lambda_\alpha$ + T $\Lambda_\beta$ + 2T $\Lambda_\gamma$ + T $\Lambda_\epsilon$ + T $\Lambda_\mu$
	d	2l	1	CA + 3CA + T $\Delta_\beta$ + T $\Delta_\gamma$ + 2T $\Delta_\delta$ + 2T $\Delta_\epsilon$ + T $\Delta_\mu$ + 2T $\Lambda_\alpha$ + T $\Lambda_\beta$ + T $\Lambda_\gamma$ + T $\Lambda_\mu$
	e	4l	3	3CA + CA + T $\Delta_\beta$ + T $\Delta_\gamma$ + 2T $\Delta_\epsilon$ + T $\Delta_\mu$ + 2T $\Lambda_\alpha$ + T $\Lambda_\beta$ + T $\Lambda_\gamma$ + 2T $\Lambda_\delta$ + T $\Lambda_\mu$
	f	3	4l	3CA + CA + T $\Delta_\beta$ + 2T $\Delta_\gamma$ + T $\Delta_\epsilon$ + T $\Delta_\mu$ + 2T $\Lambda_\alpha$ + T $\Lambda_\beta$ + 2T $\Lambda_\delta$ + T $\Lambda_\epsilon$ + T $\Lambda_\mu$

#### Rate Constants



$$\begin{array}{lll} k_1 = 5k'/16 & k_{\delta_{xx}} = k''/16 & k_{\tau_{xx}} = 9k''/48 \\ k_2 = 7k'/16 & k_{\delta_{yy}} = k''/16 & k_{\tau_{yy}} = 9k''/48 \\ k_3 = 5k''/48 & k_{\delta_{zz}} = k''/16 & k_{\tau_{zz}} = 9k''/48 \\ k_4 = 7k''/48 & k_{\delta_{xy}} = 7k''/48 & k_{\tau_{xy}} = 5k''/48 \\ k_5 = k'/16 & k_{\delta_{xz}} = 7k''/48 & k_{\tau_{xz}} = 5k''/48 \\ k_6 = 3k'/16 & k_{\delta_{yz}} = 7k''/48 & k_{\tau_{yz}} = 5k''/48 \end{array}$$

$$K_{eq} = 3k'/k''; \quad k' = k''K_{eq}/3$$

<sup>a</sup> For specification of transition states cf. Figures 5, 7, and 9 of ref 1.

attacked with equal probability by the dangling ligand. The rate constants  $k'$  and  $k''$  are defined as for other mechanisms.

The relationship between the rate constants  $k_1$ - $k_6$  and the rates of interconversion of the diastereotopic methyl groups among the eight different magnetic environments is clearly shown by the following matrix (2), whose elements are the rate constants for transferal of a nucleus in a row environment into a column en-

vironment. The exchange matrices which constitute

$$\begin{matrix} T_{xr} & T_{xs} & T_{yr} & T_{ys} & T_{zr} & T_{zs} & C_r & C_s \\ T_{xr} & k_{7xx} & k_{7xy} & k_{7yx} & k_{7xz} & k_{7zx} & k_3 & k_4 \\ T_{xs} & k_{8xx} & k_{8xy} & k_{8yx} & k_{8xz} & k_{8zx} & k_4 & k_3 \\ T_{yr} & k_{7yx} & k_{8yx} & k_{7yy} & k_{7yz} & k_{7zy} & k_3 & k_4 \\ T_{ys} & k_{8yx} & k_{7yx} & k_{8yy} & k_{8yz} & k_{8zy} & k_4 & k_3 \\ T_{zr} & k_{7zx} & k_{7xy} & k_{7yz} & k_{8zz} & k_{7zz} & k_3 & k_4 \\ T_{zs} & k_{8zx} & k_{8xy} & k_{8yz} & k_{8zz} & k_{8zz} & k_4 & k_3 \\ C_r & k_1/3 & k_2/3 & k_1/3 & k_1/3 & k_2/3 & k_3 & k_4 \\ C_s & k_2/3 & k_1/3 & k_2/3 & k_2/3 & k_1/3 & k_4 & k_3 \end{matrix} \quad (2)$$

part of the input to the line shape program are readily derived from the general matrix (2) by subtracting  $k'$  or  $k''$  from the appropriate diagonal elements to make each row sum to zero, expressing all elements in terms of  $k''$  and  $K_{eq}$  ( $= [T]/[C]$ ), and dividing all elements by  $k''$  ( $= 1/\tau$ ). As an example the exchange matrix (3) for the twist mechanism, assuming rotations about all axes are equally probable, is given below. The matrix elements were evaluated from the relationships in Table IV with  $R_r = R_p = 1/4$ . The rates of interchange of magnetic environments for a nondiastereotopic group (e.g.,  $\beta$ -H) accompanying cis-trans rearrangement can also be written in terms of  $k_1$ - $k_8$  and are given in the general matrix (4).

$$\begin{pmatrix} -1/2 & 1/8 & 0 & 1/8 \\ 1/8 & -1/2 & 1/8 & 0 \\ 0 & 1/8 & -1/2 & 1/8 \\ 1/8 & 0 & 1/8 & -1/2 \\ 0 & 1/8 & 0 & 1/4 \\ 1/8 & 0 & 0 & 1/4 \\ 0 & K_{eq}/24 & 0 & K_{eq}/24 \\ K_{eq}/24 & 0 & K_{eq}/24 & 0 \end{pmatrix} \quad (3)$$

$$\begin{matrix} T_x & T_y & T_z & C \\ T_x & \left\{ \begin{matrix} k_{6xx} + k_{7xx} & k_{6xy} + k_{7xy} & k_{6xz} + k_{7xz} & k_3 + k_4 \\ k_{6yx} + k_{7yx} & k_{6yy} + k_{7yy} & k_{6yz} + k_{7yz} & k_3 + k_4 \\ k_{6zx} + k_{7zx} & k_{6zy} + k_{7zy} & k_{6zz} + k_{7zz} & k_3 + k_4 \\ (k_1 + k_2)/3 & (k_1 + k_2)/3 & (k_1 + k_2)/3 & k_5 + k_8 \end{matrix} \right\} \\ T_y & & & \\ T_z & & & \\ C & & & \end{matrix} \quad (4)$$

The nonexchange chemical shifts of the isopropyl methyl protons of  $Al(pmhd)_3$  and  $Ga(pmhd)_3$  at temperatures above the slow-exchange regions were estimated by extrapolating the temperature dependencies of chemical shifts in these regions. The extrapolated shifts are represented by the dashed lines in Figures 3 and 4. Weighted averages of these estimated shifts reproduce the positions of the fully collapsed doublets in the fast-exchange region of  $Al(pmhd)_3$  and  $Ga(pmhd)_3$  (above 155 and 105°, respectively) within 0.4 Hz. Because of the general downfield shift with temperature of the methyl signals of  $Al(pmhd)_3$  and  $Ga(pmhd)_3$  in chlorobenzene, the error in the relative positions of the extrapolated lines should be smaller than the error in the extrapolated chemical shift of a given line. In addition, chemical shifts in the intermediate-exchange region are not extrapolated over as long a distance as are those for the fast-exchange limit. Uncertainties in relative chemical shifts in the intermediate exchange regions are not expected to exceed 0.2 Hz. Equilibrium constants at temperatures above the slow-exchange limit were calculated from the thermodynamic data in Table II.

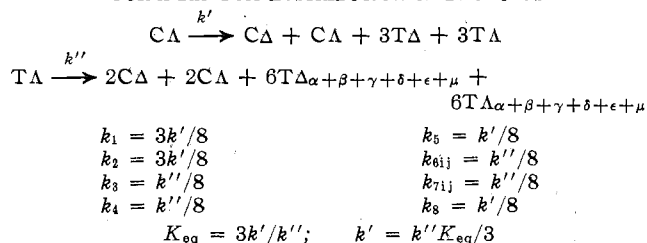
**Consideration of Mechanisms.**—The temperature dependencies of the pmr spectra of the isopropyl methyl groups over the temperature ranges 93–156° for  $Al(pmhd)_3$  and 31–105° for  $Ga(pmhd)_3$  are shown in Figures 9 and 10, respectively. Both series of spectra collapse to a single doublet with a separation of 6.9 Hz in the fast-exchange limit. This behavior indicates complete averaging of both cis-trans and r-s environ-

ments and thus requires that the rearrangement process involve both isomerization and inversion of the molecular configurations. Twists about the r- $C_3$  axis of the cis isomers and the p- $C_3$  axis of the trans isomers or bond breaking to form TBP-equatorial transition states can be eliminated as the sole reaction pathway. Twists of this type do not produce isomerization and TBP-equatorial transition states do not lead to inversion.

Considerations of the remaining mechanisms are made on the basis of comparison of experimental and computer-simulated spectra for intermediate exchange rates. No mechanism was discarded as an improbable process unless the spectra calculated for all probable assignment schemes (16 for  $Al(pmhd)_3$  and 24 for  $Ga(pmhd)_3$ ) over a reasonable range of  $\tau$  values were inconsistent with the experimental spectra. It was not considered necessary to test all assignment schemes, however, if any one produced a satisfactory fit. Three rearrangement processes definitely do not match the experimental spectra for  $Al(pmhd)_3$  and  $Ga(pmhd)_3$ : (i) a random exchange of environments, for which microscopic rate constants are given in Table VIII, (ii)

$$\begin{pmatrix} 0 & 1/8 & 0 & 1/8 \\ 1/8 & 0 & 1/8 & 0 \\ 0 & 1/4 & 0 & 1/8 \\ 1/4 & 0 & 1/8 & 0 \\ -1/2 & 0 & 0 & 1/8 \\ 0 & -1/2 & 1/8 & 0 \\ 0 & K_{eq}/24 & -K_{eq}/6 & K_{eq}/24 \\ K_{eq}/24 & 0 & K_{eq}/24 & -K_{eq}/6 \end{pmatrix} \quad (3)$$

TABLE VIII  
ISOMER DISTRIBUTION AND MICROSCOPIC RATE CONSTANTS  
FOR A RANDOM DISTRIBUTION OF PRODUCTS



bond rupture producing a 1:1 mixture of TBP-axial and TBP-equatorial transition states, and (iii) formation of SP-axial transition states which pass to products by a 1:1 mixture of primary and secondary processes. Sample spectra for  $Al(pmhd)_3$  calculated for several  $\tau$  values are compared with an actual spectrum at 128° in Figure 11. Those shown are the closest fits obtained from a series of different assignment schemes and  $\tau$  values.

Calculated spectra for the remaining mechanisms which produced the best fits to the experimental spectra are shown in Figures 9 and 10.<sup>43</sup> Spectra for the twist mechanism of  $Al(pmhd)_3$  were calculated with  $R_r = R_p = 0$ , although they are not particularly sensitive to the values of  $R_r = R_p$ . Reasonable fits were obtained

(43) The following assignment schemes produced the best fit to experimental spectra and were used in calculating the spectra in these figures.  $Al(pmhd)_3$ : twist, A; SP-primary, A; TBP-axial, B.  $Ga(pmhd)_3$ : twist, C; SP-primary, C; TBP-axial, D. The low-field component of each diastereotopic pair was assigned to s, and the high-field component, to r. (The reverse assignment, low-field component to r and high-field to s, is entirely equivalent.<sup>40</sup>) Spectra calculated for the twist mechanism of  $Al(pmhd)_3$  were found not to be very sensitive to x, y, z assignments but quite sensitive to the relative r, s assignments of components of the diastereotopic pairs. All assignments except that stated gave spectra completely inconsistent with those observed.

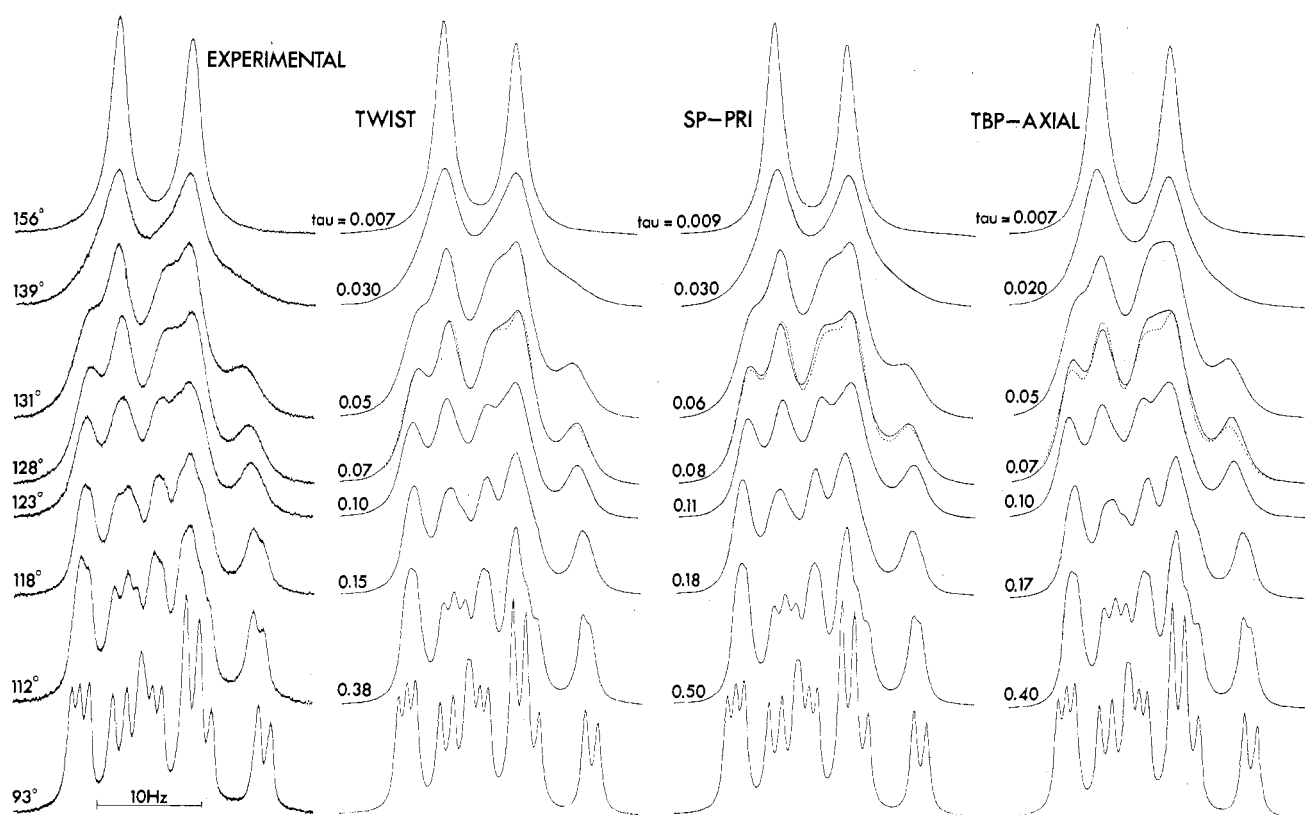


Figure 9.—Experimental methyl spectra of  $\text{Al}(\text{pmhd})_3$  in chlorobenzene and simulated spectra for various rearrangement mechanisms: twist, 100% rotation about the imaginary  $C_3$  axes of cis and trans isomers ( $R_r = R_p = 0$ , cf. Table IV); SP-PRI, SP-primary process; ·····, experimental spectrum at  $128^\circ$ .  $\tau$  values are in seconds. See also footnote 43.

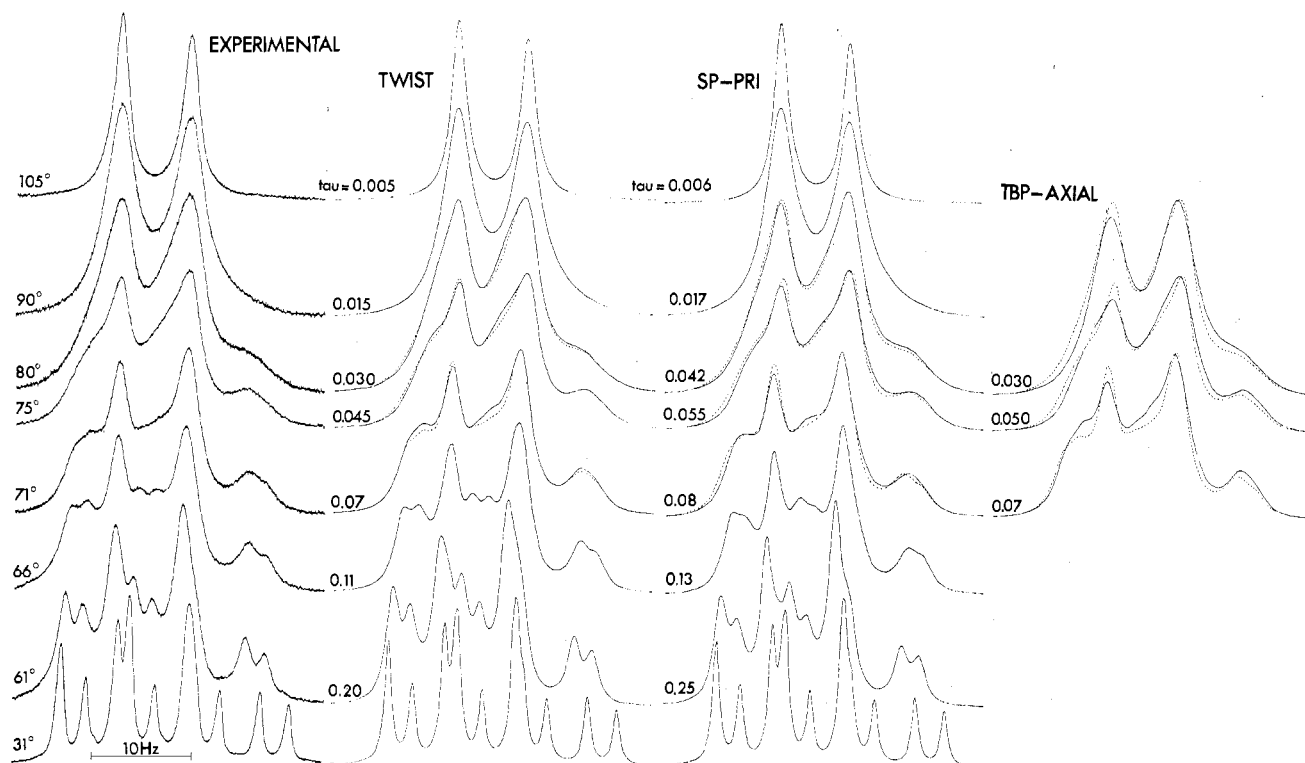


Figure 10.—Experimental methyl spectra of  $\text{Ga}(\text{pmhd})_3$  in chlorobenzene and simulated spectra for various rearrangement mechanisms: twist, 50% rotation about the real (cis) and pseudo (trans)  $C_3$  axes ( $R_r = R_p = 0.5$ , cf. Table IV); SP-PRI, SP-primary process; ·····, experimental spectra at  $71$ ,  $75$ , and  $80^\circ$ .  $\tau$  values are in seconds. See also footnote 43.

TABLE IX  
 ACTIVATION PARAMETERS<sup>a</sup> FOR THE PROBABLE REARRANGEMENT MECHANISMS OF M(pmhd)<sub>3</sub> COMPLEXES IN CHLOROBENZENE

Complex	Mechanism	Log A (sec <sup>-1</sup> )	E <sub>a</sub> , kcal/mol	ΔH <sup>‡</sup> , kcal/mol	ΔS <sup>‡</sup> , eu
Al(pmhd) <sub>3</sub>	Twist	16.18 ± 0.45	27.6 ± 1.4	26.8 ± 1.4	12.9 ± 3.5
	TBP-axial	17.62 ± 0.45	30.2 ± 1.4	29.4 ± 1.4	19.5 ± 3.5
	SP-primary	17.21 ± 0.45	29.6 ± 1.4	28.8 ± 1.4	17.6 ± 3.5
Ga(pmhd) <sub>3</sub>	Twist	13.93 ± 0.45	20.1 ± 1.2	19.4 ± 1.2	2.9 ± 3.4
	SP-primary	14.09 ± 0.45	20.5 ± 1.2	19.7 ± 1.2	3.6 ± 3.4

<sup>a</sup> The error limits quoted are estimated standard deviations calculated from weighted least-squares best fits to Eyring and Arrhenius equations and include an assumed error of ±20% in  $\tau$  values. The actual errors in  $\tau$  values estimated from the range of acceptable  $\tau$ 's for a given temperature are less than ca. 5%, but the error range was increased in order to take into account possible errors in chemical shift extrapolations (Figures 3 and 4) and errors in  $K_{eq}$  (Table II).

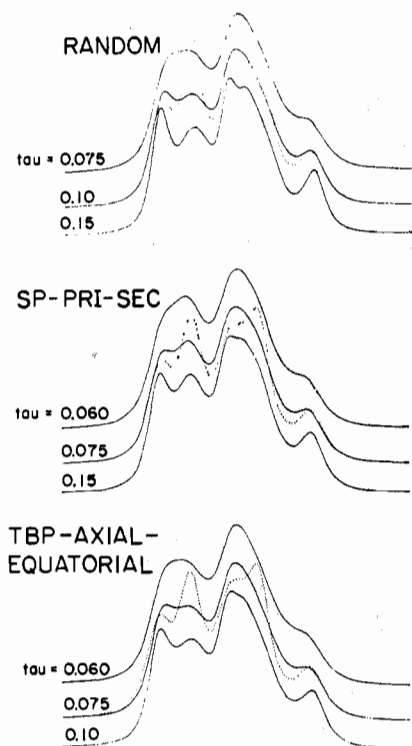


Figure 11.—Experimental methyl spectrum (····) of Al(pmhd)<sub>3</sub> in chlorobenzene at 128° compared to certain rearrangement mechanisms: SP-PRI-SEC, 1:1 mixture of SP-primary and SP-secondary processes; TBP-AXIAL-EQUATORIAL, 1:1 mixture of TBP-axial and TBP-equatorial transition states.  $\tau$  values are in seconds. The spectral comparisons indicate that the three mechanisms do not match the experimental spectrum.

over the range  $0 \leq R_r = R_p \leq 0.5$ . In the case of Ga(pmhd)<sub>3</sub> the best fit to a twist process was obtained with  $R_r = R_p = 0.5$ , but reasonable fits were achieved over the interval  $0.25 \leq R_r = R_p \leq 0.75$ . Rearrangement through SP-axial transition states by the primary process only results in spectral fits which are as satisfactory, or nearly as satisfactory, as those for the twist pathways. Spectra for the TBP-axial process of Al(pmhd)<sub>3</sub> give an apparently poorer agreement with experimental results than do the preceding two mechanisms. However, the extent of discrepancy is not considered large enough for elimination of this mechanism. Variation of  $K_{eq}$  values to the limits allowed by experimental error (cf. Table II) resulted in a considerably improved fit. For Ga(pmhd)<sub>3</sub> a similar variation of the equilibrium constant did not substantially improve the fit.

On the basis of the line shape analysis the most probable rearrangement mechanisms for both Al(pmhd)<sub>3</sub> and Ga(pmhd)<sub>3</sub> are certain twist processes or a bond rup-

ture process involving SP-axial transition states which pass to products by the primary process. Although a pathway requiring TBP-axial transition states must be included as possible for the aluminum complex, it is considered less probable than the above two pathways. Least-squares plots fitting the kinetic data for these mechanisms to the Eyring equation (5) are shown in Figure 12. Activation parameters are listed in Table IX.

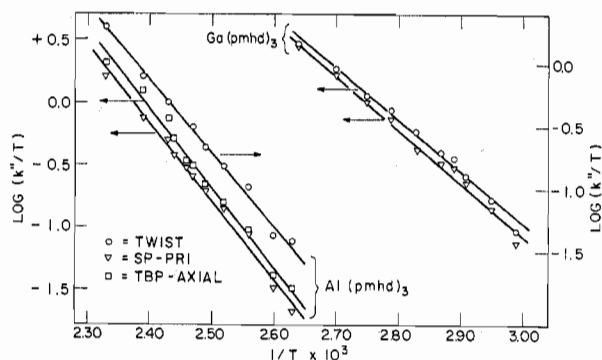


Figure 12.—Eyring plots for intramolecular rearrangements of Al(pmhd)<sub>3</sub> and Ga(pmhd)<sub>3</sub> in chlorobenzene solution: left, twist, SP-primary, and TBP-axial for Al(pmhd)<sub>3</sub>; right, twist and SP-primary for Ga(pmhd)<sub>3</sub>.

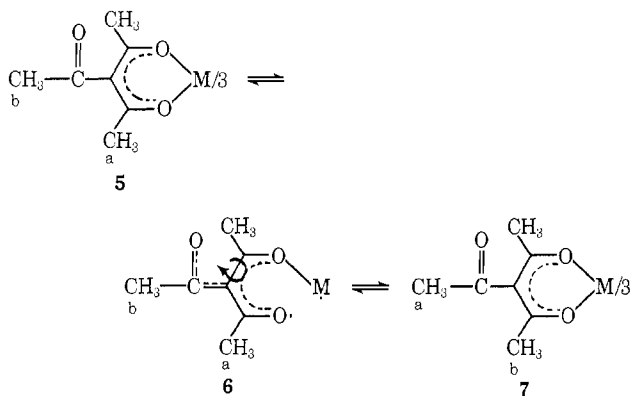
$$1/\tau = (kT/h) \exp(\Delta S^\ddagger/R - \Delta H^\ddagger/RT) \quad (5)$$

Activation parameters for Ga(pmhd)<sub>3</sub> are comparable to those obtained for the exchange of methyl environments in Ga(acac)<sub>2</sub>(hfac) and Ga(acac)<sub>2</sub>(dbm), for which  $E_a = 14.5, 20.6$  kcal/mol and  $\Delta S^\ddagger = 1.7 \pm 4.4, 3.5 \pm 8.0$  eu, respectively.<sup>23</sup> Data for the latter complex, measured in benzene, are more relevant since tfac and hfac complexes undergo rearrangements faster than their nonfluorinated analogs.<sup>7,9,23</sup> Equivalent data for aluminum complexes are presently unavailable, although Fay and Piper<sup>7</sup> reported activation energies of 23.5 and 20.8 kcal/mol for the isomerization of Al(tfac)<sub>3</sub> and Ga(tfac)<sub>3</sub>, respectively. However, these values were obtained from exchange rates at coalescence assuming the same preexponential factor ( $\log A = 15.19$ ) as for Co(tfac)<sub>3</sub>. The results of Fortman and Sievers<sup>9</sup> for rearrangements of mixed-ligand aluminum complexes of acac, hfac, and dipivaloylmethane in chlorobenzene are in considerable disagreement with the data for Al(pmhd)<sub>3</sub>. Pinnavaia, *et al.*<sup>23</sup> have pointed out that Fortman and Sievers did not take into account temperature dependence of chemical shifts at slow exchange. Consequently, their activation parameters are presumably not reliable.

It has been suggested elsewhere<sup>6,9</sup> that a twist mechanism should be associated with low preexponential

factors and negative activation entropies. This suggestion is consistent with the  $\Delta S^\ddagger$  values for rearrangements of  $\text{Co}(\text{mhd})_3^1$  (1) (*ca.* +7 eu) and  $\text{Co}(\text{bzac})_3^{44}$  (*ca.* +10 eu) in chlorobenzene, which proceed by a bond rupture (TBP-axial) pathway, and of  $\text{Fe}(\text{S}_2\text{CNR}_2)_2\text{-}[\text{S}_2\text{C}_2(\text{CF}_3)_2]$  complexes,<sup>29</sup> which invert by a twist process.<sup>45</sup> It would imply that a bond rupture pathway is operative for  $\text{Al}(\text{pmhd})_3$  and perhaps also for  $\text{Ga}(\text{pmhd})_3$ . Unfortunately, it is not yet clear that this suggestion has any general validity. Racemization of  $\text{Cr}(\text{C}_2\text{O}_4)_3^{3-}$  and  $\text{Cr}(\text{en})(\text{C}_2\text{O}_4)_2^-$  in water proceeds by one-ended bond rupture, yet low preexponential factors ( $\log A = 8.05, 8.09$ , respectively) are found,<sup>46</sup> implying negative activation entropies (*ca.* -27, -24 eu). Twist processes have been implicated in the racemization of  $\text{Fe}(\text{phen})_3^{2+}$ <sup>47</sup> and  $\text{Co}(\text{EDTA})^-$ <sup>48</sup> in aqueous solution, for which rather large positive activation entropies have been found (+21 eu for the pH-independent path of both). Several groups<sup>47-49</sup> have also suggested that a negative activation entropy should be related to a dissociative mechanism. Although  $\Delta S^\ddagger$  values for a given rearrangement mechanism in aqueous and weakly polar organic solvents may differ in magnitude and/or sign, there are clearly not enough cases for which mechanisms are firmly established in either type of solvent to permit the use of activation entropies and preexponential factors as reliable indicators of mechanism.

In an attempt to estimate values of activation parameters expected for a bond rupture process, the  $\text{M}(\text{triac})_3$  complexes **5**,  $\text{M} = \text{Al}, \text{Ga}$ , were prepared and their pmr spectra were investigated in chlorobenzene from 30 to 180°. The only pmr-detectable process



would be linkage isomerization ( $5 \rightleftharpoons 7$ ), which interchanges methyl groups a and b *via* a five-coordinate intermediate. The spectra of these complexes at 30° consist of two sharp signals of 2:1 intensity separated by *ca.* 0.23 ppm. At 180° no evidence of line broadening was observed. Simulated spectra allow a conservative estimate of 0.05 sec as the shortest preexchange lifetime compatible with the experimental spectra. Using activation parameters for the bond

(44) A. Y. Girgis and R. C. Fay, *J. Amer. Chem. Soc.*, **92**, 7061 (1970).

(45) Large negative activation entropies have also been reported for the rearrangement of  $\text{Ti}(\text{acac})_2(\text{OR})_2$  complexes, which are suggested (but not proven) to proceed by a twist mechanism: D. C. Bradley and C. E. Holloway, *J. Chem. Soc. A*, 282 (1969).

(46) E. Busbra and C. H. Johnson, *ibid.*, 1937 (1939).

(47) F. Basolo, J. C. Hayes, and H. M. Neumann, *J. Amer. Chem. Soc.*, **76**, 3807 (1956).

(48) D. W. Cooke, Y. A. Im, and D. H. Busch, *Inorg. Chem.*, **1**, 13 (1962).

(49) I. A. W. Shimi and W. C. E. Higginson, *J. Chem. Soc.*, 260 (1958); M. L. Morris and D. H. Busch, *J. Phys. Chem.*, **63**, 340 (1959).

rupture mechanism (SP-primary) which best fits both pmhd complexes, the preexchange lifetimes at 180° were calculated as  $1.2 \times 10^{-3}$  and  $6.6 \times 10^{-5}$  sec for  $\text{Al}(\text{pmhd})_3$  and  $\text{Ga}(\text{pmhd})_3$ , respectively. Thus rearrangement of the former is at least 40 times and of the latter at least 760 times faster than linkage isomerization of the corresponding  $\text{M}(\text{triac})_3$  species. If the behavior of  $\text{Al}(\text{triac})_3$  and  $\text{Ga}(\text{triac})_3$  parallels that of  $\text{Co}(\text{triac})_3^{17}$  linkage isomerization will have a higher activation energy than other intramolecular rearrangements (which for cobalt(III) involve, at least in an operational sense, bond rupture<sup>1,44</sup>), and rate differences will be even larger at the lower temperatures at which coalescence is observed for  $\text{Al}(\text{pmhd})_3$  and  $\text{Ga}(\text{pmhd})_3$ . Qualitative pmr studies of aluminum and gallium mixed triac-acac complexes in chlorobenzene suggest that these species undergo rearrangement processes with coalescence temperatures slightly lower than those of the corresponding pmhd complexes. On this basis triac complexes are not significantly different kinetically from acac and pmhd complexes. Although we cannot exclude possible large differences in solvation or electronic effects between triac and acac, especially in the transition state, the above results imply that a bond rupture mechanism is not operative for  $\text{Ga}(\text{pmhd})_3$  but are inconclusive for  $\text{Al}(\text{pmhd})_3$ . The data of Klabunde and Fay<sup>17</sup> indicate that inversion is 16 times faster than linkage isomerization of  $\text{Co}(\text{triac})_3$  at 90° in chlorobenzene.

**Scandium Complexes.**—Attempts to examine the rearrangement reactions of  $\text{Sc}(\text{pmhd})_3$  were unsuccessful. This complex exhibited single  $\beta$ -H and isopropyl methyl doublet signals in chlorobenzene and at temperatures as low as -95° in dichloromethane. The spectrum of  $\text{Sc}(\text{triac})_3$  coalesced to a single resonance in chlorobenzene at 60°. Addition of free ligand or  $\text{Sc}(\text{acac})_3$  showed that coalescence is due to rapid intermolecular ligand exchange, and this process was not further studied. Equimolar mixtures of  $\text{Sc}(\text{pmhd})_3$  and  $\text{Sc}(\text{acac})_3$  in chloroform below 40° revealed two acac, two pmhd  $\beta$ -H, and two isopropyl methyl doublet resonances, consistent with slow ligand exchange and rapid environmental averaging in the mixed-ligand complexes and  $\text{Sc}(\text{pmhd})_3$ .

### Summary

The pmr results described above demonstrate that the rearrangement reactions of  $\text{Al}(\text{pmhd})_3$  and  $\text{Ga}(\text{pmhd})_3$  in chlorobenzene are intramolecular and involve both isomerization and inversion. Line shape analysis of the isopropyl methyl signals leads to exclusion of the following pathways as the sole reaction mechanism for either complex: (a) twists about the real (cis) or pseudo (trans)  $C_3$  axes only; (b) bond rupture producing TBP-equatorial transition states; (c) bond rupture producing a mixture of TBP-axial and TBP-equatorial transition states;<sup>50</sup> (d) bond rupture with formation of SP-axial transition states and products by a 1:1 mixture of primary and secondary processes; (e) a random scrambling of ligand environments; (f) for  $\text{Ga}(\text{pmhd})_3$ , bond rupture producing TBP-axial transition states. The following

(50) Only a 1:1 mixture was thoroughly tested in the line shape analysis of both complexes. Note that limiting mechanisms (b) and (f) were excluded for  $\text{Ga}(\text{pmhd})_3$ , and for  $\text{Al}(\text{pmhd})_3$  mechanism (b) was eliminated while a TBP-axial pathway (f) was considered only less probable.

pathways are allowed on the basis of the line shape analysis: (g) twist mechanisms involving less than ca. 50% and from ca. 25 to 75% rotation about the real and pseudo  $C_3$  axes of  $Al(pmhd)_3$  and  $Ga(pmhd)_3$ , respectively; (h) bond rupture with formation of SP-axial transition states and products by the primary process; (i) for  $Al(pmhd)_3$ , bond rupture producing TBP-axial transition states.

The estimate that linkage isomerization of  $Ga(triac)_3$  is at least  $1/800$  times as fast as rearrangement of  $Ga(pmhd)_3$  is interpreted to mean that the bond rupture path (h) is unlikely for the latter. A similar argument for  $Al(pmhd)_3$  is inconclusive and the significant difference in activation entropies and preexponential factors between the two complexes is consistent with the possibility that different mechanisms may be involved. If a bond rupture process were common to the rearrangements of these complexes, the rates would be expected to parallel the average M-O bond energies. The only available bond energies are derived from calorimetric measurements of  $M(acac)_3$  complexes. For homolytic fission the mean Al-O and Ga-O bond energies are 63 and 48 kcal/mol.<sup>51</sup> The mean Sc-O bond energy is reported to be 67 kcal/mol.<sup>52</sup> To the extent that these bond energies are accurate and are applicable in the present context, it is seen that the rearrangement rates of  $M(pmhd)_3$  do not correlate with them. Ionic size appears to be a more important

determinant of rate. Pauling's ionic radii for tripositive Al, Ga, and Sc are 0.50, 0.62, and 0.81 Å, respectively, which is the order of increasing rearrangement rates of  $M(pmhd)_3$  complexes. Rearrangement rates in two other series of complexes,  $M(tfac)_3$ <sup>7</sup> (M = Al, Ga, In) and  $M(acac)_2X_2$ <sup>38,53</sup> (M = Ti, Zr, Hf), appear to follow a similar order. Increased ionic size should decrease steric interactions and facilitate a twist mechanism.

The most important conclusions from the present investigation are presented in the list of excluded and allowed rearrangement mechanisms given above. The arguments just given and the activation parameters in Table IX do not lead to an unambiguous selection of only one of the allowed mechanisms for each complex. The fundamental question as to whether a bond rupture or a twist mechanism is operative cannot, unfortunately, be answered by the results of this study. Investigation of other aluminum complexes, whose properties may permit a clear distinction between twist and bond rupture rearrangement pathways by line shape analysis is under way.<sup>54</sup>

**Acknowledgment.**—This research was supported by the National Science Foundation under Grant GP-7576X. We thank Dr. R. C. Fay for a preprint of ref 44 prior to its publication, Dr. G. M. Whitesides for valuable discussions, and Mrs. Sandra Eaton for checking rate constant relationships.

(51) R. J. Irving and G. W. Walter, *J. Chem. Soc. A*, 2690 (1969).  
 (52) J. L. Wood and M. M. Jones, *Inorg. Chem.*, **3**, 1553 (1964).

(53) T. J. Pinnavaia and R. C. Fay, *ibid.*, **7**, 502 (1968).  
 (54) J. R. Hutchison, R. H. Holm, and E. L. Muetterties, work in progress

CONTRIBUTION FROM THE DEPARTMENT OF CHEMISTRY  
 AND THE RADIATION LABORATORY,<sup>1</sup> UNIVERSITY OF NOTRE DAME, NOTRE DAME, INDIANA 46556

## Mössbauer Spectra of Tin(IV) Complexes of Picolinic and Pyridine-2,6-dicarboxylic Acids

By DATTA V. NAIK AND COLUMBA CURRAN\*

Received June 8, 1970

Mössbauer and infrared spectra have been obtained for a series of tin(IV) complexes containing two picolinate groups, for chloro- and bromotris(picolinato)tin(IV), for di-*n*-butyl(dipicolinato)tin(IV), and for the monohydrates of diphenyl(dipicolinato)tin(IV) and bis(dipicolinato)tin(IV). Quadrupole splittings indicate a trans arrangement of C-Sn-C bonds in all  $R_2Sn(pic)_2$  and  $R_2Sn(dipic)$  compounds except diphenylbis(picolinato)tin(IV). A comparison of the isomer shifts of tin(IV) complexes with picolinic acid and 8-hydroxyquinoline reveal a much greater tin s character for trans than for cis C-Sn-C bonds.

Mössbauer spectra of complexes of picolinic acid and pyridine-2,6-dicarboxylic acid (dipicolinic acid) with tin(II) have been reported from this laboratory.<sup>2</sup> Many more varied complexes of tin(IV) with these acids can be prepared and it is of interest to learn something about the electron distribution in these complexes and their configuration from Mössbauer spectra.

It is also of interest to compare tin complexes of picolinic acid with those of 8-hydroxyquinoline. Both sets

of complexes contain five-membered



rings. The smaller isomer shift obtained for  $Sn(ox)_2$  than for  $Sn(pic)_2$ <sup>2</sup> suggests that the electrons of the ring O-Sn bond are more effective than those of the COO-Sn bond in shielding the outer unshared tin electrons. The greater variety of tin(IV) complexes affords a more extensive comparison of the O-Sn bonds in these complexes.

(1) The Radiation Laboratory is operated by the University of Notre Dame under contract with the Atomic Energy Commission. This is AEC Document No. COO-38-736.

(2) M. A. Doskey and C. Curran, *Inorg. Chim. Acta*, **3**, 169 (1969).